2022

The age of shear zones on western King Island

Authors: R.F. Berry, R. Bottrill, G.V. Cumming, J.L. Everard and K. Goemann

Date: 07/2022

Email: info@mrt.tas.gov.au
Website: www.mrt.tas.gov.au

REPORT No: TR31

Geological Survey Technical Report 31

Tasmanian Government

Mineral Resources Tasmania
Department of State Growth

Geological Survey Technical Report 31:

The age of shear zones on western King Island

by R.F. Berry, R. Bottrill, G.V. Cumming, J.L. Everard and K. Goemann

Cover: View northward to Cataraqui Point from Seal Rocks with the Currie Shear Zone extending along the coast. The photo shows exposures of breccia, cataclasite and mylonite which abut, and are derived predominantly from, the Loorana Granite (positioned to the east).

Abstract

Several shear zones occur within Neoproterozoic granites on the north and west coasts of King Island. We have applied the chemical U-Th-Pb dating method to monazite and xenotime from five of these shear zones to show that they were formed at 740 ± 9 Ma, immediately after granite intrusion. The strongest reactivation on the shear zones occurred at 500 Ma and was probably associated with sinistral movement. This event may have occurred at the same time as the regional cleavage was developed in the Grassy Group. Further reactivation occurred during the Devonian. There is evidence for brittle reactivation of the Disappointment Bay West Shear Zone in the early Permian that may correlate with movement on the Grassy River Fault and possibly sinistral transpression on the eastern margin of Gondwana.

Tasmanian Government

Mineral Resources Tasmania

Department of State Growth
www.mrt.tas.gov.au

The age of shear zones on western King Island

by R.F. Berry[1], R. Bottrill[2], G.V. Cumming[2], J.L. Everard[2] and K. Goemann[3]
[1]*Centre for Ore Deposit and Earth Sciences - University of Tasmania*
[2]*Geological Survey Branch - Mineral Resources Tasmania*
[3]*Central Science Laboratory - University of Tasmania*

CONTENTS

FIGURES

TABLES

1.0 Introduction

Numerous mylonitic and cataclastic zones have been reported from the Neoproterozoic Cape Wickham and Loorana Granites which are well-exposed on the north and west coasts of King Island (Cox, 1973; Streit, 1994; Streit and Cox, 1998) and have more recently been mapped by MRT at 1:25,000 scale (Everard, 2011; Calver and Everard, 2012; Everard and Calver, 2013a, b).

Monazite, which is common in these granites, is partially recrystallised in shear zones at temperatures below the closure temperature and is therefore a very useful mineral for the dating of mylonitic rocks (Oriolo et al., 2018). The aim of this project is to use chemical U-Th-Pb dating methods to constrain the age of the shear zones of King Island. In this report the group terms monazite, rhabdophane, florencite, allanite, xenotime, etc are used but the specific species here are most probably always monazite-Ce, rhabdophane-Ce, florencite-Ce, allanite-Ce and xenotime-Y.

2.0 Regional geology

Mesoproterozoic metasedimentary rocks, mainly turbidites, underlie most of King Island (Figure 1). Two distinct formations have long been recognised: the Surprise Bay and Fraser Formations (e.g. Gresham, 1972). The western sequence, the Surprise Bay Formation (Berry et al., 2005; Calver and Everard, 2014) forms a north-south-striking, tightly to isoclinally folded belt up to 8 km wide, extending the full length of King Island, from Stokes Point to Cape Wickham. It consists of at least 3 km thickness of mainly quartzofeldpathic and pelitic schist, quartzite, micaceous quartzite and rare thin calcareous lenses. The typical mineral assemblage in the schists is quartz +muscovite +biotite (±plagioclase ±garnet ±K feldspar ±andalusite). A lower-grade, strongly sheared correlative is exposed on the coast near Currie. The depositional age of the Surprise Bay Formation is constrained between the youngest detrital zircons (3 grains at 1350 ± 90 Ma; Black et al., 2004) and a metamorphic monazite age of 1287 ±18 Ma (Berry et al., 2005).

The eastern sequence, the Fraser Formation (Direen and Jago, 2008) largely consists of thick-bedded or laminated, micaceous, fine-grained quartz sandstone, siltstone and grey to black mudstone. Although less deformed and mostly of lower metamorphic grade than the Surprise Bay Formation, garnet, biotite and amphibole are locally present, particularly in the core of the central "Lymwood Anticline" (Calver, 2012). The youngest detrital zircons in a sample from Naracoopa are 1444 ± 12 Ma (Black et al., 2004). Similarities in protolith and detrital zircon distribution (Black et al., 2004) led Calver (2012) to propose a correlation with the Surprise Bay Formation.

Several large amphibolite bodies, derived from intrusions of tholeiitic basalt composition, occur within the Fraser Formation near Pegarah, and smaller intrusions are widespread in the Surprise Bay Formation. A body near Cape Wickham has been dated at ~1370 Ma (U-Pb, zircon) by J. Mulder (pers. comm.).

D1 and amphibolite facies regional metamorphism of the Surprise Bay Formation, and by correlation the Fraser Formation, occurred at ~1290 Ma, based on U-Pb dating of authigenic monazites from southern King Island (Berry et al., 2005). J. Mulder (pers. comm.) reported a U/Pb (LA-ICP-MS) monazite age of 1300 ±14 Ma for the metamorphism.

These Mesoproterozoic, predominantly metasedimentary sequences were intruded by syn-deformational granitoids (Cox, 1973; Turner et al., 1998; Calver et al., 2013). In the north of the island, the Cape Wickham Granite (760 ±12 Ma, Turner et al., 1998) is a dominantly medium-grained K-feldspar-porphyritic, biotite monzogranite to alkali feldspar granite. Late minor intrusions of more mafic granodiorite, and more felsic leucogranite, aplite and pegmatite are locally present. A poorly exposed tract of Surprise Bay Formation separates the Cape Wickham Granite from the Loorana Granite (Everard, 2014), a north-south trending body extending along the west coast from Cataraqui Point to the New Year Islands. The Loorana Granite (748 ±2 Ma; Black et al., 1997) is slightly less felsic than the Cape Wickham Granite. Two felsic porphyry sills, intruding the Surprise Bay Formation near Currie, were dated at 776 ± 6 and 772 ± 7 Ma (Calver et al., 2013). The granite intrusions were probably synchronous with the D2 event in the Cape Wickham region (Cox, 1973). Several mylonite and cataclasite zones occur within these granites (Streit, 1994; Streit and Cox, 1998), and are the principal subject of this report.

In the southeast of King Island, the Fraser Formation is unconformably overlain by the Grassy Group, which consists of an east-dipping succession of conglomerate, siltstone, diamictite, dolostone, limestone and shale, with uppermost mafic volcanic rocks (Scott, 1951; Waldron and Brown, 1993) dated at ~ 635- 580 Ma (Calver, 2012; Mulder et al., 2020). The Grassy Group was deformed and metamorphosed to low greenschist facies in the Cambrian (Calver, 2012; Meffre et al., 2004).

Numerous tholeiitic metadolerite sills and dykes, some up to 20 m thick, intrude both the Surprise Bay Formation and the Neoproterozoic granites throughout King Island. Attempts to date them have been unsuccessful, but they may be related to the Ediacaran (~ 580 Ma) volcanism in the upper Grassy Group.

The effects of the Cambrian Tyennan Orogeny (~514-506 Ma; Corbett et al., 2014 and references therein) and Middle Devonian Tabberabberan Orogeny (~389 Ma; Black et al., 2005) are difficult to identify or separate on King Island due to the lack of Early Palaeozoic rocks.

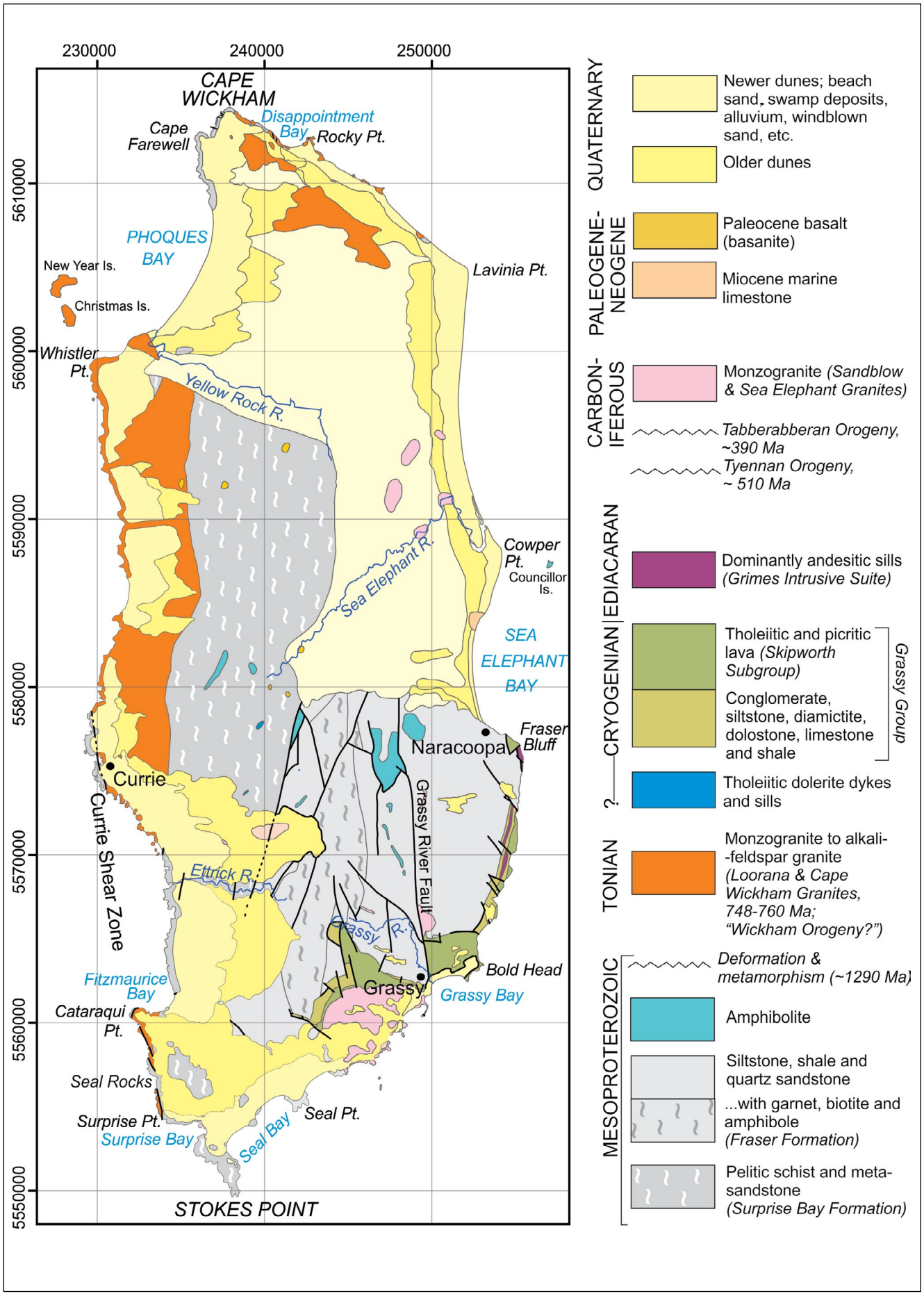

Figure 1. Geological map of King Island (geology from Everard, 2011; Calver and Everard, 2012; Everard and Calver 2013a, 2013b).

In the east of King Island, the Fraser Formation and Grassy Group are intruded by the Sandblow (formerly Grassy) and Sea Elephant Granites, which are small bodies of biotite +-hornblende monzogranite. The former is dated at 350.8 ± 1.7 Ma (U-Pb SHRIMP on zircon; Black et al., 2005). An undeformed felsic porphyry dyke near Currie yielded a U/Pb SHRIMP age of 350.5 ± 4.3 Ma (Black et al., 1997).

3.0 Previous work

The structure of fault zones along the north coast (Cape Wickham Shear Zone, Disappointment Bay Shear Zone, Rocky Point Shear Zone) and the west coast (Currie Shear Zone) were extensively studied by Streit (1994) and Streit and Cox (1998). They reported steeply-dipping shear zones containing mylonites, from 10 to 30 m-wide along the north coast with the mineralogy quartz + albite + alkali feldspar + biotite + muscovite ± epidote ± titanite. The Cape Wickham mylonites formed at temperatures of approximately 460 °C and are dominated by K loss. Further east, the Disappointment Bay (West) Shear Zone had a final movement at a lower temperature (310 °C) based on the quartz and K feldspar $\delta^{18}O$ values, and had significant mass gain, mostly quartz.

The Currie Shear Zone is a mylonite belt 60 m wide with extensive overprinting by cataclastic events related to brittle faults (Streit, 1994). Retrograde alteration produced a lower greenschist facies mineral assemblage of quartz + albite + alkali feldspar + chlorite + epidote + titanite within these mylonites, which are finer grained than the north coast examples. Narrow fault zones cut the mylonite and nearby granite and these faults contain multiple generations of cataclasite. The cataclasite has high Na_2O/Al_2O_3 values and is depleted in K_2O (< 1 wt%) relative to the original granite.

The Currie Shear Zone extends to Cataraqui Point (Streit, 1994) and then on to Surprise Point (Everard, 2011). Holm (2002) reported a fine-grained quartz-white mica-biotite-tourmaline schist from Surprise Point, which is strongly foliated and preserves evidence of a complex deformation history. Holm analysed some REE phosphate grains from this sample, including five large (30 μm) monazite grains, which retained the magmatic age of the Loorana Granite, 769 ± 44 Ma. Most of the analysed grains were smaller, 10-15 μm, with rounded to euhedral shapes that had low totals, near 90%, typical of rhabdophane.

Streit (1994) and Streit and Cox (1998) reported K/Ar biotite ages from the shear zones that were much younger, 350 to 460 Ma, than the granite intrusion age but interpreted these as regional cooling ages and conclude the shear zones formed in an earlier regional -scale fluid infiltration event at mid crustal depth.

There are many radiometric cooling ages reported from King Island (22 K/Ar biotite, 6 K/Ar muscovite, 1 K/Ar hornblende, 4 Rb/Sr muscovite, 7 titanite fission track, 12 apatite fission track) covering a range of closure temperatures (Table 1). These have been combined with granite ages, and geological evidence for uplift and erosion, to identify the T-t path for the island (Figure 2). The Rb/Sr muscovite ages from McDougall and Leggo (1965), as recalculated for Streit (1994), show rapid cooling to below 500 ºC (Figure 2) by 724 Ma at Cape Wickham, and 735 Ma at Ettrick River. At Ettrick River the cooling continued to below 350 °C (K/Ar muscovite closure) by 725 Ma. With the 660 Ma unconformity surface only a few kilometres away (Calver, 2012), we conclude the whole area cooled to about 100 °C (2-4 km depth) very quickly. At Cape Wickham, the K/Ar muscovite ages have been variably reset to a range in age from 610 Ma to 500 Ma. This is consistent with reheating to near the K/Ar muscovite closure temperature during metamorphism in the Cambrian. All K/Ar biotite age measurements for King Island are reset to less than 500 Ma supporting the conclusion of Meffre et al. (2004) that the Cambrian regional metamorphism on King Island reached low greenschist facies (350-400 °C).

K/Ar biotite and titanite fission track ages have similar closure temperatures (Table 1). These retain a wide range of ages on King Island from 460 Ma to 300 Ma (McDougall and Leggo, 1965; Streit, 1994; Gleadow and Lovering, 1978a), which may be due to slow cooling, or perhaps a second thermal pulse during the Devonian metamorphism and granite emplacement (Sandblow Granite at 351 Ma, Black et al., 2005). Apatite fission track ages (Gleadow and Lovering, 1978a) indicate the central part of King Island cooled to 100 °C by 250 Ma but the east and west coast reached this temperature 100 million years later. Gleadow and Lovering (1978a) concluded that the distribution of these ages required movement on the Grassy River Fault after 200 Ma.

Table 1. Closure temperatures for radiogenic systems that are not disturbed by recrystallisation. Adapted from Oriolo et al. (2018), Carlson (2011), Eberlei et al. (2015), Coyle and Wagner (1998) and Gleadow and Lovering (1978b).

U-Pb Zircon	>700 °C
U-Th-Pb Monazite	>700 °C
K/Ar Hornblende	450-550 °C
Rb-Sr Muscovite	400-550 °C
K/Ar Muscovite	310-430 °C
K/Ar Biotite	270-350 °C
Titanite fission track	250-330 °C
Apatite fission track	60-120 °C

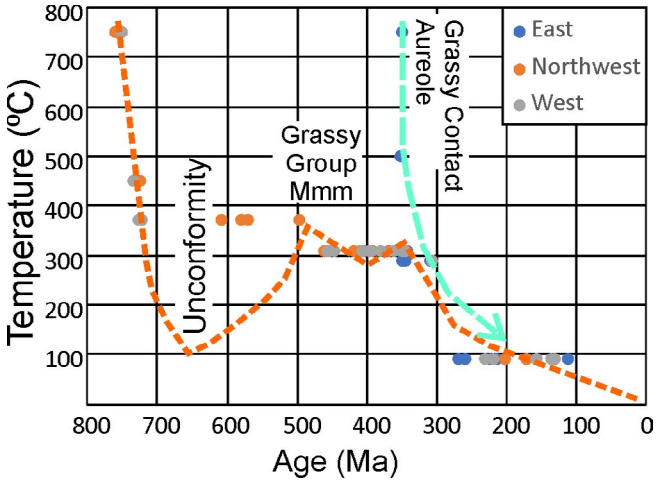

Figure 2. Cooling path for King Island granitoids, in orange, based on the radiometric dating and geological controls. See text for sources of data.

4.0 Methods

The chemical U-Th-Pb dating method is commonly used to determine the age of minerals which contain significant amounts of U and Th, such as zircon, monazite and xenotime. Numerous studies of isotopic systems have shown that the Pb in these minerals was derived from radiogenic decay of Th and U and can be used to calculate the length of time elapsed since the mineral was formed (Montel et al., 2018). Monazite typically contains less than 1 ppm common Pb at the time of crystallisation.

Traditionally U, Th and Pb have been measured using mass spectrometers, in which the minimum spot size (area to be analysed) is ~10 µm diameter. This type of measurement is, however, unsuitable for the grains detected in this project, which are small and have complex textural relationships. Electron probe micro-analysis (EPMA) can routinely measure Pb, U and Th with a detection limit near 50 ppm on electron beams with 1 micron diameter, and an analysis volume about 3 µm in diameter, in monazite and xenotime (Montel et al., 2018). The grains can be quickly located using automated "rare phase search" based on back scattered electron (BSE) detectors, and the location of the analytical volume can be controlled very accurately.

Samples from shear zones were collected from coastal outcrops by G. V. Cumming and J. L. Everard during detailed geological mapping of King Island between 2009 and 2021. Some were collected specifically for this project. Sample locations are shown in Appendix 1. Standard thin sections were prepared and a subset of 18 samples chosen for detailed study using polished blocks or polished thin sections. Most samples were examined petrographically and by X-ray diffraction. Not all proved suitable for dating by the U-Pb technique; for example, samples from the Disappointment Bay East Shear Zone and the shear zone at Cataraqui Point either did not contain REE-phosphates, or did not produce meaningful results (e.g. grains were too small, too low in Th, or had very low totals).

Polished samples were coated with 20 nm of carbon using a HHV Auto306 carbon evaporator. Automated mineral analysis was used to locate grains of zircon, monazite and xenotime using a FEI MLA 650 scanning electron microscope (SEM), with a combination of backscattered electron (BSE) mapping to find high mean atomic number grains, and energy dispersive X-ray spectroscopy (EDS) to identify grains of interest (Sack et al., 2011). EPMA was conducted at the Central Science Laboratory, University of Tasmania, on a JEOL JXA-8530F Plus instrument equipped with 5 wavelength-dispersive x-ray spectrometers at 16 kV accelerating voltage. The beam current and beam diameter was varied as required for specific spots. The "Probe For EPMA" software package by Probe Software Inc. (Eugene, OR, USA) was used for data acquisition and quantification with the default matrix correction algorithms (Armstrong/Love Scott, LINEMU). The U, Th, and Pb background intensity was determined by fitting an exponential curve to multiple background measurements on both sides of the peak (Jercinovic et al., 2012). For all other elements a mean atomic number background correction was performed (Donovan and Tingle, 1996), which involves using calibration curves acquired on standard reference materials instead of measuring background intensities. A range of spectral interference corrections were applied as part of the matrix correction procedure (Donovan et al., 1993). All elements were acquired in differential PHA mode to minimise high order spectral interferences. Detailed conditions for analysis are given in Appendix 2, along with the successful monazite analyses. Mn, Er and Yb were below detection level in all monazite analyses and are not reported. Analytical results from xenotime are shown in Appendix 3.

The errors quoted in this work represent the error associated with counting statistics. They do not include any systematic errors associated with calibration, or the errors in decay constants. The calibration is continually checked against SHRIMP analysed standards and reproduces the SHRIMP ages to within error. We conclude the sum of the calibration errors is less than 1% in the age. For individual spot analysis the error quoted is the 1σ error. For the weighted mean age, a 95% confidence interval is used.

A particular problem in this project has been the separation of monazite from rhabdophane. Rhabdophane is a hydrous REE phosphate with a composition very similar to monazite (Nagy and Draganits, 1999; Nagy et al., 2002). The major difference is that rhabdophane is hydrous and can incorporate significant common Pb at formation. The formula is reported as $CePO_4 \cdot H_2O$ or $CePO_4 \cdot nH_2O$,where n= 0.5 to 1.0. The theoretical water content is 7.1 wt% with n=1 and 3.7 wt.% with n=0.5. In this report we will follow the approach of

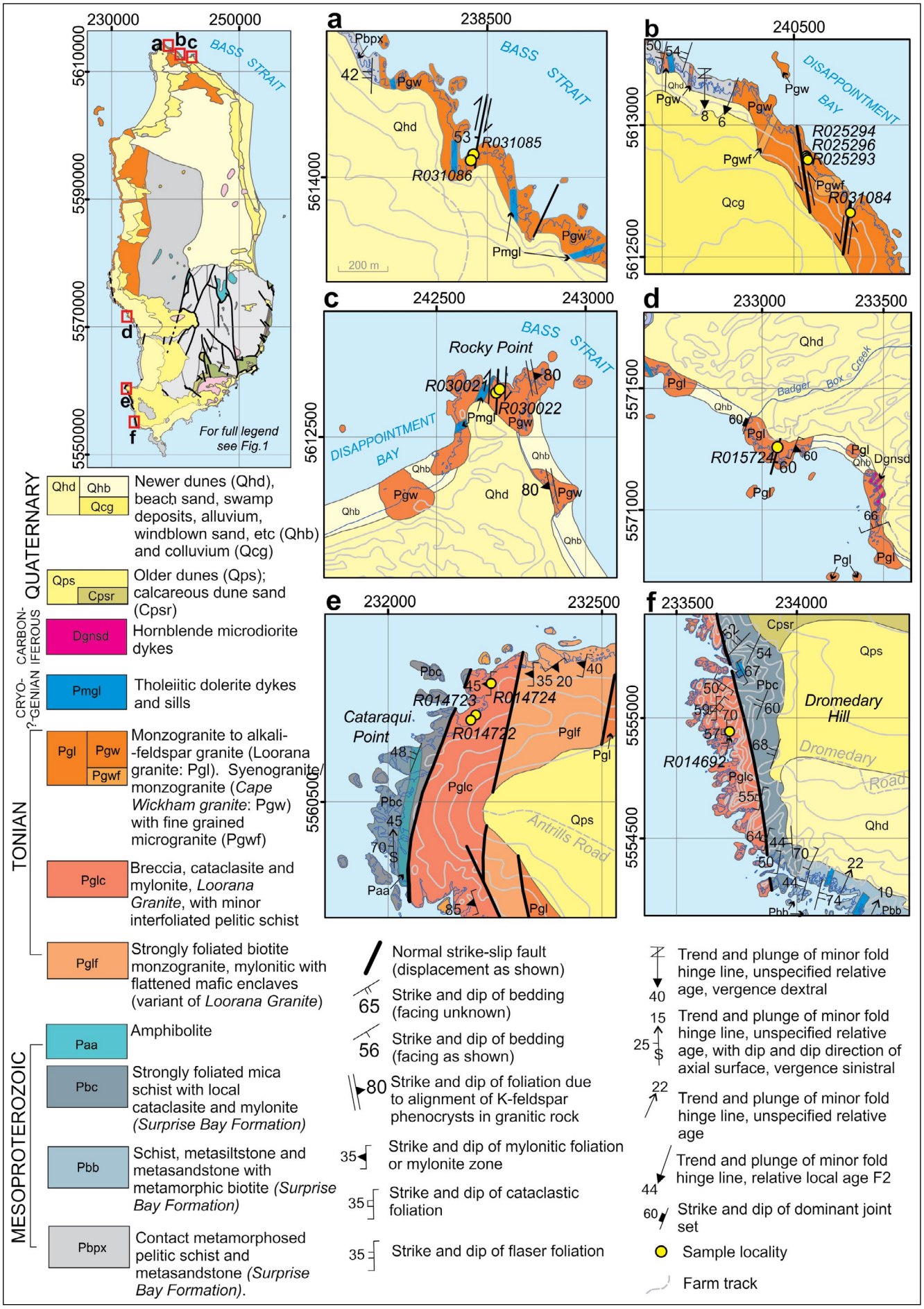

Figure 3. Location maps a-f for samples discussed in this report. See summary map for position of these maps. Geology from Everard, 2011; Calver and Everard, 2012; Everard and Calver 2013a, 2013b. Note that no samples were successfully dated from the Currie Shear Zone at Cataraqui Point (e).

Nagy et al. (2002) and report the analyses with totals 97.5-102% as monazite. Rhabdophane commonly has a low closure temperature, and commonly contains less U and Th than monazite.

The BSE/ SEM rare phase search was carried out on 18 samples to locate monazite grains. However, this method cannot discriminate between monazite and rhabdophane, and as a result there were many grains analysed with totals of 94-97.5% which we regard as Type 2 (n=0.5) rhabdophane (Rh2) and 88- 94% as Type 1 (n=1) rhabdophane (Rh1). All the analytical results were closely inspected for low totals or other evidence of contamination. Analyses with Mg >0.2%, Al>0.3%, K>0.2% and Ca>2% were discarded. From the eight samples containing monazite, 174 analyses were accepted from 266 measurements. Most of the discarded analyses were interpreted as rhabdophane. From the 18 samples, only eight produced valid monazite analyses. One sample, R015724, was found to contain xenotime. The xenotime grains were very small and complex but suitable for chemical U-Th-Pb age determination by EPMA. Rhabdophane was particularly common in samples from the Currie Shear Zone.

5.0 Results

5.1 Cape Wickham Shear Zone

The Cape Wickham Shear Zone crops out on the north coast of King Island, ~700 m SE of Cape Wickham (Figure 3a). It dips moderately west (mylonitic fabric dipping ~53°to 290°) and has an oblique normal displacement with a dextral strike-slip component. The eastern contact against porphyritic Cape Wickham Granite (with K-feldspar phenocrysts aligned parallel to the mylonite) is sharp and is followed to the west by 0.5 -1.5 m of laminated mylonite, which passes further west into progressively less foliated granite (Streit and Cox, 1998; J. L. Everard field notes).

5.1.1 Sample R031085 (ultramylonite)

Sample R031085, collected from the core of the shear zone, ~1m from the western contact, is a quartz-albite-K-feldspar rich ultramylonite (<1% porphyroclasts, <0.3 mm diameter) with a small amount of brown biotite. Fe-Ti oxides are replaced by epidote and titanite. Albitisation is nearly complete. The white mica defines a foliation in a recrystallised, relatively equant matrix

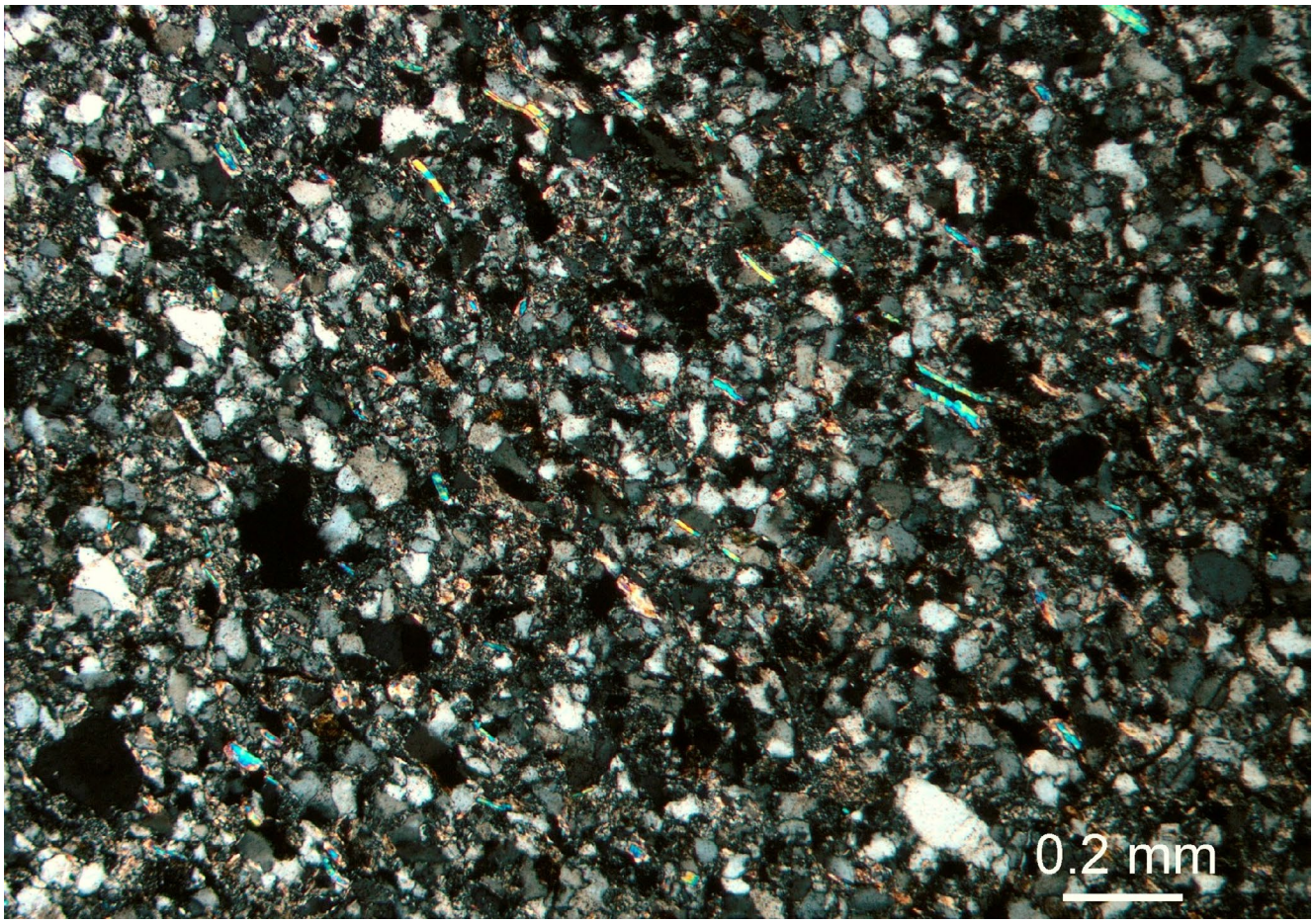

Figure 4. Texture of sample R031085 (crossed polarised light) showing microporphyroclasts of albite in annealed matrix with weakly aligned muscovite.

of quartz and feldspar (Figure 4). This is typical of mylonite in which grain boundary migration (GBM) was active at the end of deformation (Kirschner et al., page 474 in Snoke et al., 1998). Grujic et al. (2011) argued that grain boundary migration in quartz is the dominant mechanism above 500ºC. The near complete recrystallisation of feldspar is consistent with this estimate of the temperature during deformation.

Ultramylonite R031085 contained 180 monazite grains (largest 80 micron, 11 over 20 μm width). Twenty successful analyses were carried out on five grains. Six analyses are probably inherited grains (Figure 5a) with high Y and Th, typical of high temperature formation, and crystallisation ages of 1690 Ma to 810 Ma. Ten analyses have high Y (1.3-2.2%), high Th (5.1-6.5%) and relatively consistent U (0.2-0.3%). These grains give a weighted age of 762 ± 15 Ma (MSWD=1.7). The remaining analysis has a slightly lower Y, lower Th, lower U and a nominal age of 600 Ma. The textural evidence shows that grain 6 (Figure 6a) is deformed and cracked. Grain 2 has been largely replaced except in the intact core. Grains 1 and 4 show little evidence of strain. In the cracks and on rims, the monazite has largely reacted to allanite with minor REE carbonates.

5.1.2 Sample R031086 (strongly foliated granite)

Sample R031086 is a strongly foliated porphyritic granite collected from the less deformed western part of the shear zone, about 10m west of the mylonite. The mineralogy is similar to the ultramylonite R031085, with khaki biotite stable in a relatively coarse-grained foliated granitic texture (Figure 7). The plagioclase is broken. The microcline is extensively replaced by white mica around the margins. The original large quartz grains have been flattened and now form medium-grained quartz aggregates with an inequigranular interlobate texture consistent with dominant grain boundary migration during deformation. There are extensive micaceous bands that are finer grained.

Six hundred monazite grains were detected with the largest at 40 μm (621 particles, 11 over 20 μm). Many of the grains are cracked (Figure 6b) with little evidence of healing of cracks. The monazite is rimmed by allanite, rhabdophane and apatite with minor REE carbonates.

Nineteen valid analyses were collected from five grains. Two analyses with high Y and Th, indicate inherited ages, 810 and 840 Ma, that produce a bump on the kernel density plot (Figure 5b). The remaining 17 grains have typical monazite compositions for granite (0.9-2.1% Y, high Th, 0.1-0.7% U) and give a weighted mean age of 752 ±17 Ma (MSWD= 3.6). The high MSWD and complex shape of the kernel density plot suggest there is more spread in the ages than explainable by inheritance alone. The peak in the curve at 730 Ma could be interpreted as a partial reset of some monazite ages, or perhaps the deformation age is only slightly younger than the intrusion age.

5.1.3 Summary

The magmatic age for foliated granite R031086 is perhaps expected for a rock with relatively low strain on the margin of the Cape Wickham Shear Zone. The age distribution for ultramylonite R031085 is more problematic. This appears to be the highest strain mylonite studied and was probably deformed at the highest temperature based on the GBM-type texture. Streit and Cox (1998) report the $\delta^{18}O$ values of three minerals (quartz, K feldspar, biotite) in the mylonite and estimate the metamorphic temperature as 456 ±12ºC. There should be significant resetting of the monazite during deformation. There are two possible solutions. Monazite may have been unstable so there was no healing of broken and deformed grains. Alternatively, the regional cooling curve (Figure 2) suggests that the Cape Wickham area cooled below 460 °C by 720 Ma and never reached this temperature again. The most realistic interpretation is that the shear zone formed soon after the granite intrusion. We conclude the younger peak in the monazite kernel density plot at 730 Ma reflects the age of deformation in the Cape Wickham Shear Zone.

5.2 Disappointment Bay West Shear Zone

The westernmost shear zone at Disappointment Bay (~800 m NNW of the car park) is 10-15m wide and dips west (Figure 3b). On both sides, coarse-grained Cape Wickham Granite passes into foliated granite and then mylonite. Bands of porphyroclast-rich and porphyroclast-poor mylonite occur across the zone with narrow (30 cm thick) bands of ultramylonite dipping 65°/265° (Figure 8). Streit and Cox (1998) report the $\delta^{18}O$ values of quartz and K feldspar from the mylonite in this shear zone and calculated a deformation temperature of 306 ± 29 °C. The reported structure is sinistral strike slip (Streit and Cox, 1998). A much narrower (~0.3 m) mylonite band with similar fabric (dipping ~42° to 265°) occurs a few metres away on the eastern side of the main shear zone.

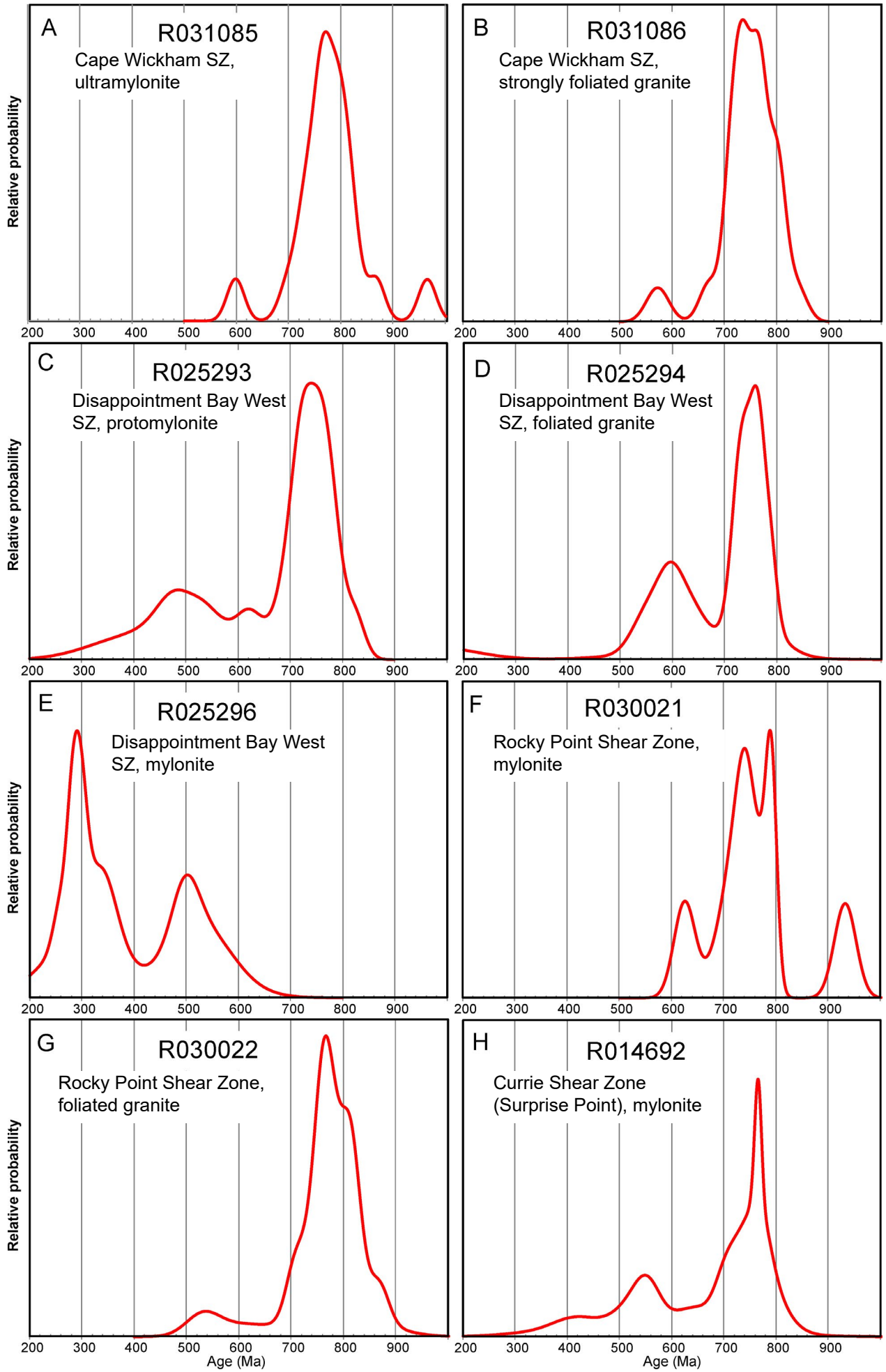

Figure 5. Probability density plot for monazite grains: Cape Wickham SZ A. R031085 B. R031086; Disappointment Bay West SZ C. R025293, D. R025294, E. R025296. Rocky Point SZ F. R030021, G. R030022. Currie SZ H. R014692.

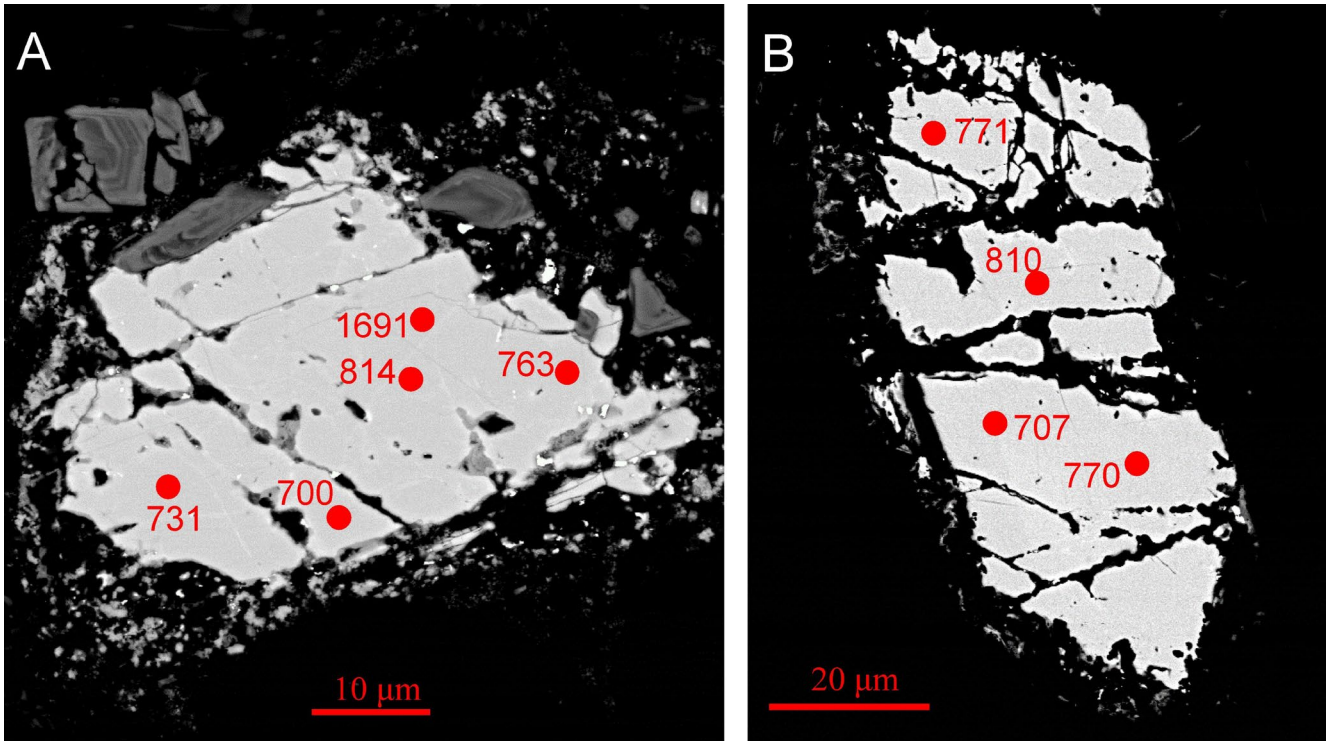

Figure 6. BSE image of: A: grain 6 in sample R031085. B: of grain 9 in sample R031086. Ages shown near analytical spots in red.

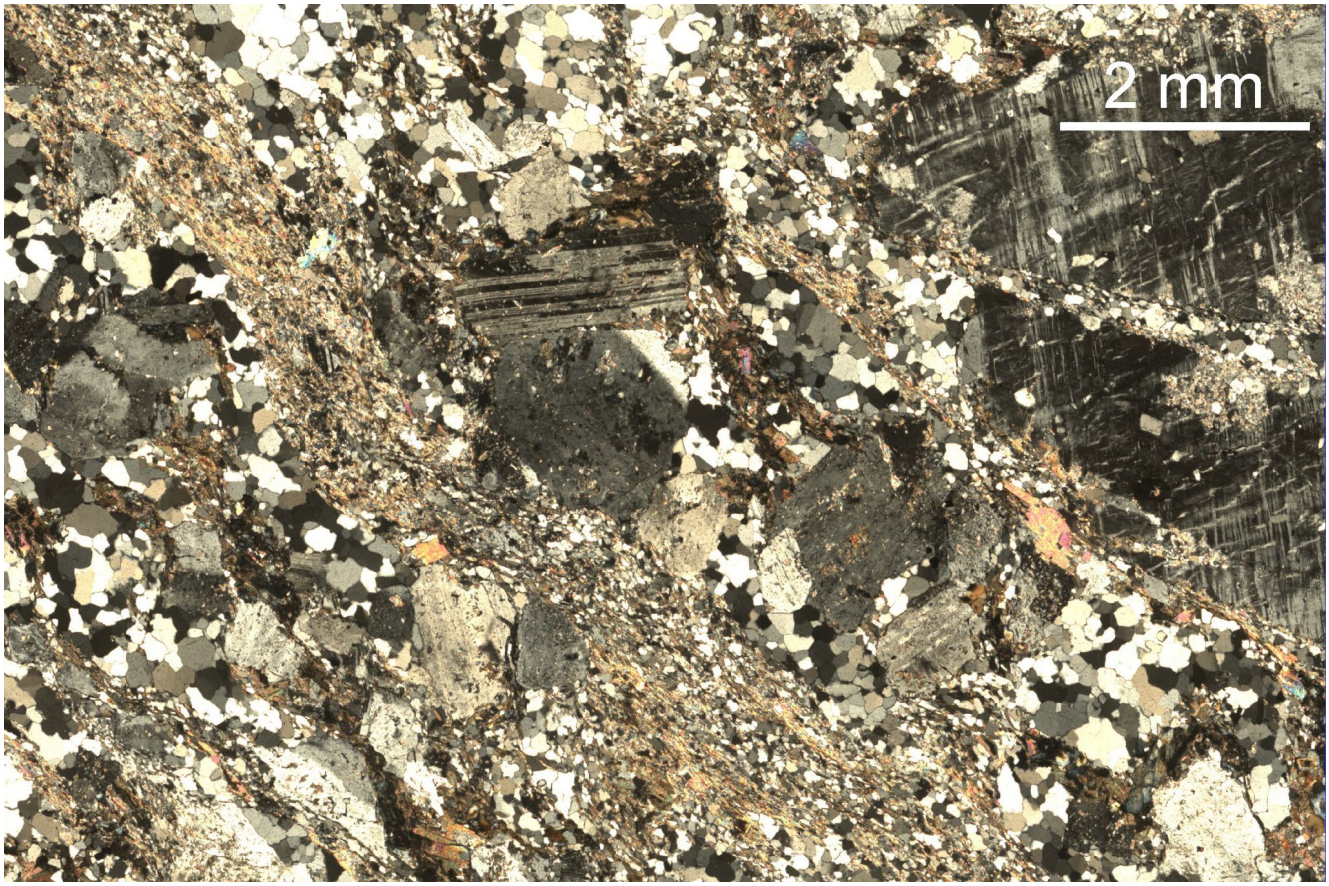

Figure 7. Texture of sample R031086 (cross polarised light). Large microcline grain cracked with mica replacement around the rims and along cracks. Quartz in deformed patches 200 µm wide that are probably deformed igneous quartz grains. Grain size of mica quartz bands is about 100 µm.

Figure 8. Banded coarse and fine grained, mylonitized granite west of Disappointment Bay.

5.2.1 Sample R025293 (protomylonite)

Sample R025293 is a protomylonite with fractured feldspar as porphyroclasts in a complexly deformed matrix of quartz and mica. In thin section (Figure 9), 1 mm albite porphyroclasts are common in a foliated groundmass of quartz and muscovite. Biotite and chlorite are common. Biotite in the matrix is green, suggesting formation at low T. Very little coarse K feldspar remains, but is common in the matrix (from XRD analysis). Quartz shows evidence of bulge nucleation. There are bands of coarser quartz (50-100 μm) and much finer grained bands of quartz (20-30 μm).

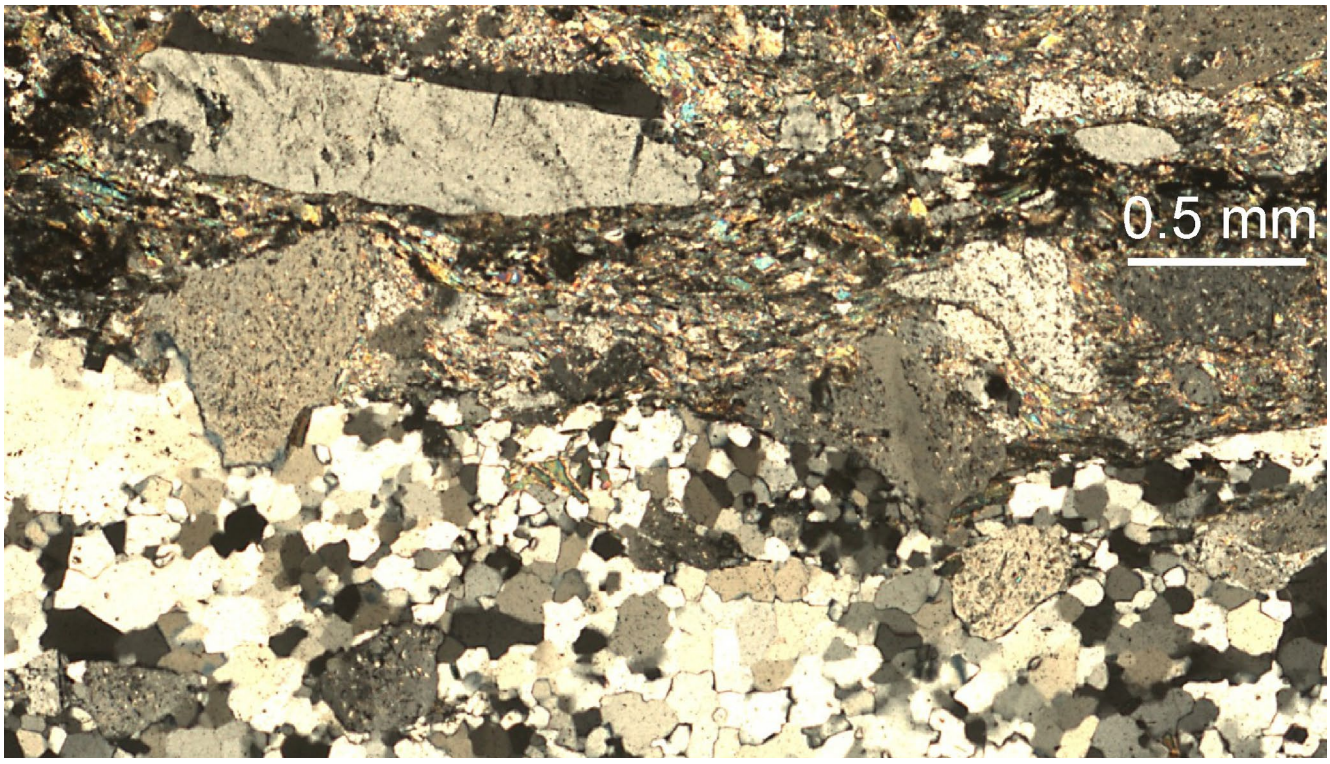

Figure 9. Texture of sample R029293 (cross polarised light), showing porphyroclasts of feldspar in foliated mica and recrystallised quartz matrix.

One hundred and seventy grains of monazite were found, with the largest 100 µm across, and 30 grains over 20 µm width. From these, 43 valid analyses were carried out on seven grains. Two analyses were older than the granite age. Twenty four analyses retain a magmatic age (Figure 5c). These have Y contents 0.7 to 1.7%, and are mostly high Th and very low U. They give a weighted mean age of 747 ±11 Ma (MSWD=1.7) for the granite. Seventeen analyses have been at least partially reset to lower ages. These generally have much lower Y, and variable Th (1.4-5 %). They have higher LREE than the analyses with ages over 700 Ma. The most common age of reset grains is 500 Ma but there is also a tail to younger ages indicating a reset event no older than 400 Ma. The ages match the monazite texture. Undeformed grains such as grain 6 (Figure 10a) retain the magmatic age, but grains that have been microboudinaged with evidence of healing such as grain 5 (Figure 10b), have a variable age reflecting the resetting by recrystallisation.

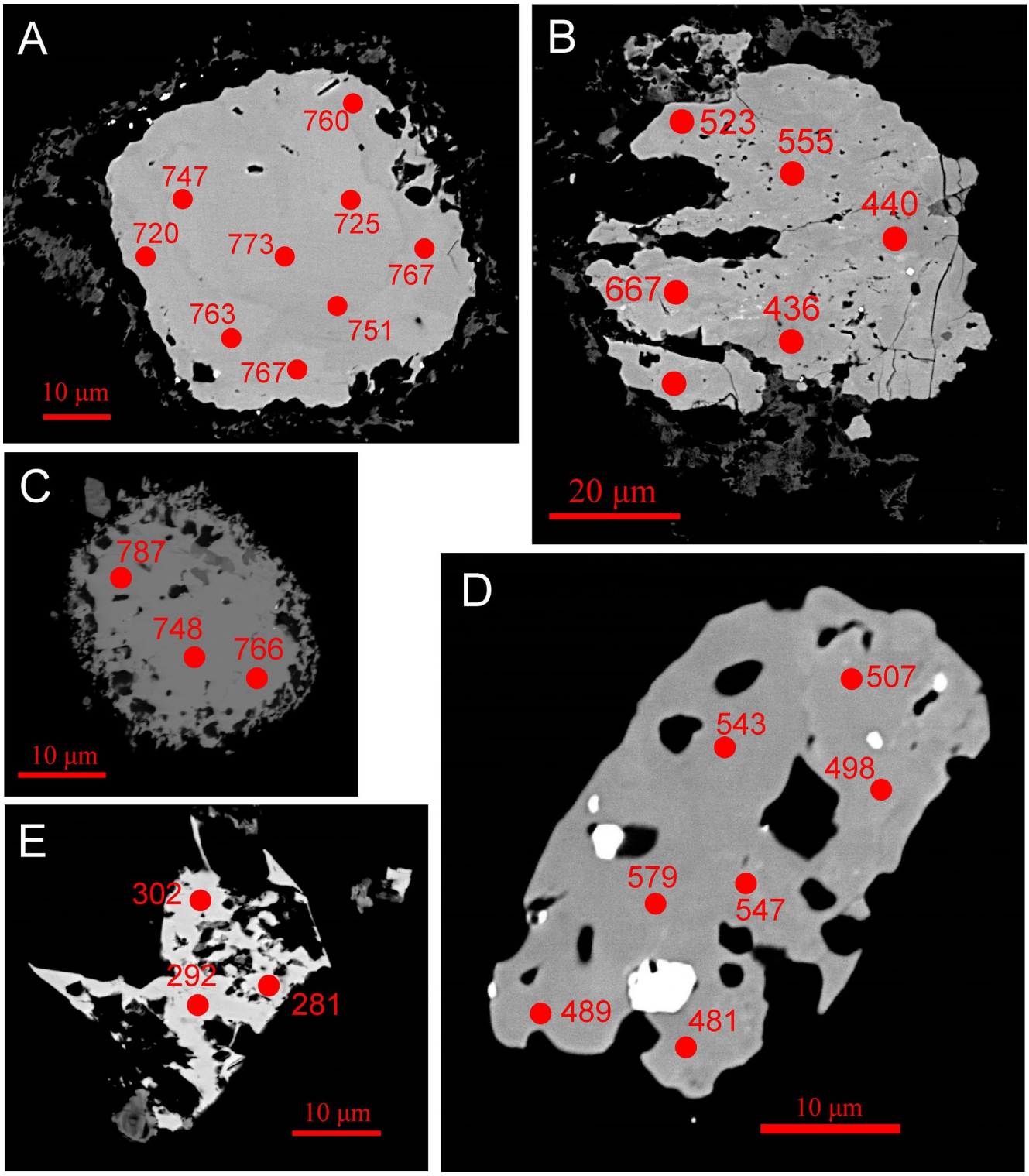

Figure 10. BSE image of monazite in Disappointment Bay West Shear Zone: A. magmatic grain 6 in sample R025293. B. grain 5 in sample R025293. Microboudinage monazite grain showing evidence for healing of cracks and extensive recrystallisation; C. grain 1 in sample R025294. Equidimensional and highly corrode monazite with retention of magmatic age; D. annealed grain 3 in sample R025296; E. grain 8 in sample R025296. High U monazite skeleton possibly reflecting the removal of Th and LREE by a hydrothermal event. Ages in Ma shown near analytical spots in red.

5.2.2 Sample R025294 (foliated granite)

Sample R025294 is a moderately oxidised, coarse-grained foliated granite from adjacent to the shear zone. It has a deformed granite texture (Figure 11) with relict porphyroclasts (up to 2 mm). The matrix is largely recrystallised quartz and K-feldspar (grain size 80-100 µm) and there is limited undulose extinction in the quartz. The alteration mineralogy is albite-muscovite-pyrite. Titanite and epidote were not detected and the allanite content is lower than in protomylonite R025293. Rare relict biotite is heavily chloritised. Kaolinite is present but may be due to weathering. Rhabdophane is present.

The rare phase search identified 274 grains of monazite, with the largest 80 µm long, and 23 grains over 20 µm. Fifteen valid analyses were measured on seven grains (Figure 5d). Grain 1 (Figure 10c) shows little evidence of strain but is very corroded around the margins and has mostly magmatic ages. Other grains are variously broken and recrystallised with variable retention of magmatic age. Nine analyses with 0.3 to 2% Y gave a typical granite age of 756 ±17 Ma (MSWD =1.9). Five grains with Y <1% contribute to a peak at 600 Ma which is interpreted as a partial reset age. One analysis with 0.3% Y, and low Th and U gives a Mesozoic age with a very large error.

5.2.3 Sample R025296 (mylonite)

Sample R025296 is a mylonite from a 30 cm wide foliated zone within the shear zone. The texture is a very fine-grained quartz and muscovite with 10% feldspar porphyroclasts (0.2 to 1.5 mm). Within the matrix texture there are discrete bands of very fine-grained (5-20 µm) material (Figure 12). Sharp breaks in the texture appear to be brittle fractures and some of these offset late pyritic veins. The dominant mineralogy is albite-quartz-K-feldspar-muscovite with very little chlorite. Biotite was not detected. No titanite, epidote or allanite were detected, and rutile is the main Ti-bearing mineral. Florencite and rhabdophane are common.

Four hundred grains of REE phosphate were found, with the largest 50 µm across, and 13 grains over 20 µm. However, many of these were rhabdophane. From the valid monazite analyses, two distinct ages were found (Figure 5e). Eight analyses, mainly from grain 3 (Figure 10d) with Y of 0.2 to 1.1% typical of low temperature growth, and with 2.4 to 4.5% Th, very low U, and normal REE patterns, have a weight average age of 511 ±25 Ma (MSWD =0.69).

Figure 11. Texture of sample R029294 (cross polarised light), showing porphyroclasts of feldspar and recrystallised quartz.

Figure 12. Texture of sample R029296 (cross polarised light), showing porphyroclasts of feldspar in very fine matrix of quartz and mica. Late Fe oxide (after pyrite) veins are offset along discrete fractures parallel to the foliation.

Fourteen analyses from grains 3, 7, 8 and 9, have a weighted average age of 293 ±15 Ma. (MSWD=2.1). Most of these grains have high U (>0.3%) compared to <0.05% U in the Cambrian analyses (Figure 13). Grain 8 (Figure 10e) has very high U (>1%) and a LREE-depleted composition. The high U grains have a skeletal texture interpreted here as relict from hydrothermal corrosion of an original larger monazite. The evidence for post mylonite brittle deformation and veining is compatible with this young age. This is the first time that a Permian fault movement has been identified by radiometric dating in Tasmania.

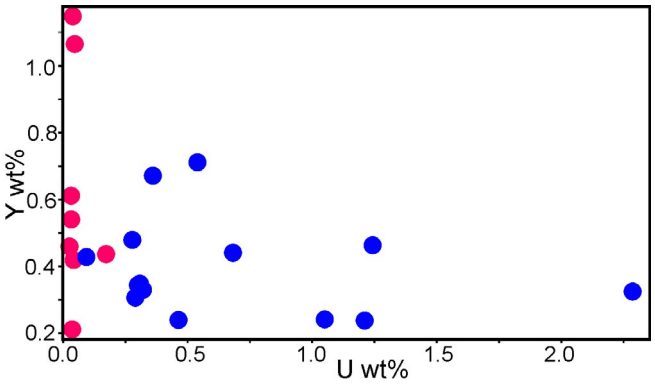

Figure 13. U vs Y for monazite from sample R025296. Red is for 500 Ma and blue is for 300 Ma analyses.

The Grassy River Fault is along strike from, and parallel to, the Disappointment Bay West Shear Zone (Figure 1). It strikes 350° and is steeply dipping. The fault has a kilometre scale offset of the Sandblow Granite (Calver, 2012) and must be younger than 350 Ma. It is very likely the hydrothermal event recorded in mylonite R025296 is associated with brittle reactivation of the shear zone associated with movement on the Grassy River Fault.

5.2.4 Summary

The host magmatic age for Disappointment Bay West Shear Zone is 750 Ma. The high MSWD of the "magmatic" analyses is the only evidence that the shear zone may have been initiated close the age of the granite intrusion. There is extensive later resetting of monazite in this shear zone. A ductile deformation probably occurred at 500 Ma. The textures include bulge nucleation which is typical of low greenschist facies (Grujic et al., 2011). From protomylonite R029293 and mylonite R029296 the most likely ductile age is 500 Ma. This is similar to the peak age for metamorphism of the Grassy Group (Figure 1). The 600 Ma peak in the kernel density plot for foliated granite R029294 is interpreted as a partial reset rather than another faulting event. A brittle deformation event associated with veining occurred at 300 Ma and may correlate with movement on the Grassy River Fault further south.

5.3 Rocky Point Shear Zone

The Rocky Point Shear Zone is located in a small gulch on the eastern headland of Disappointment Bay, ~260 m NE of the beach (Figure 3c). It occurs within dominantly coarse-grained porphyritic granite. The shear zone is relatively narrow (<3 m wide), and dips mod-

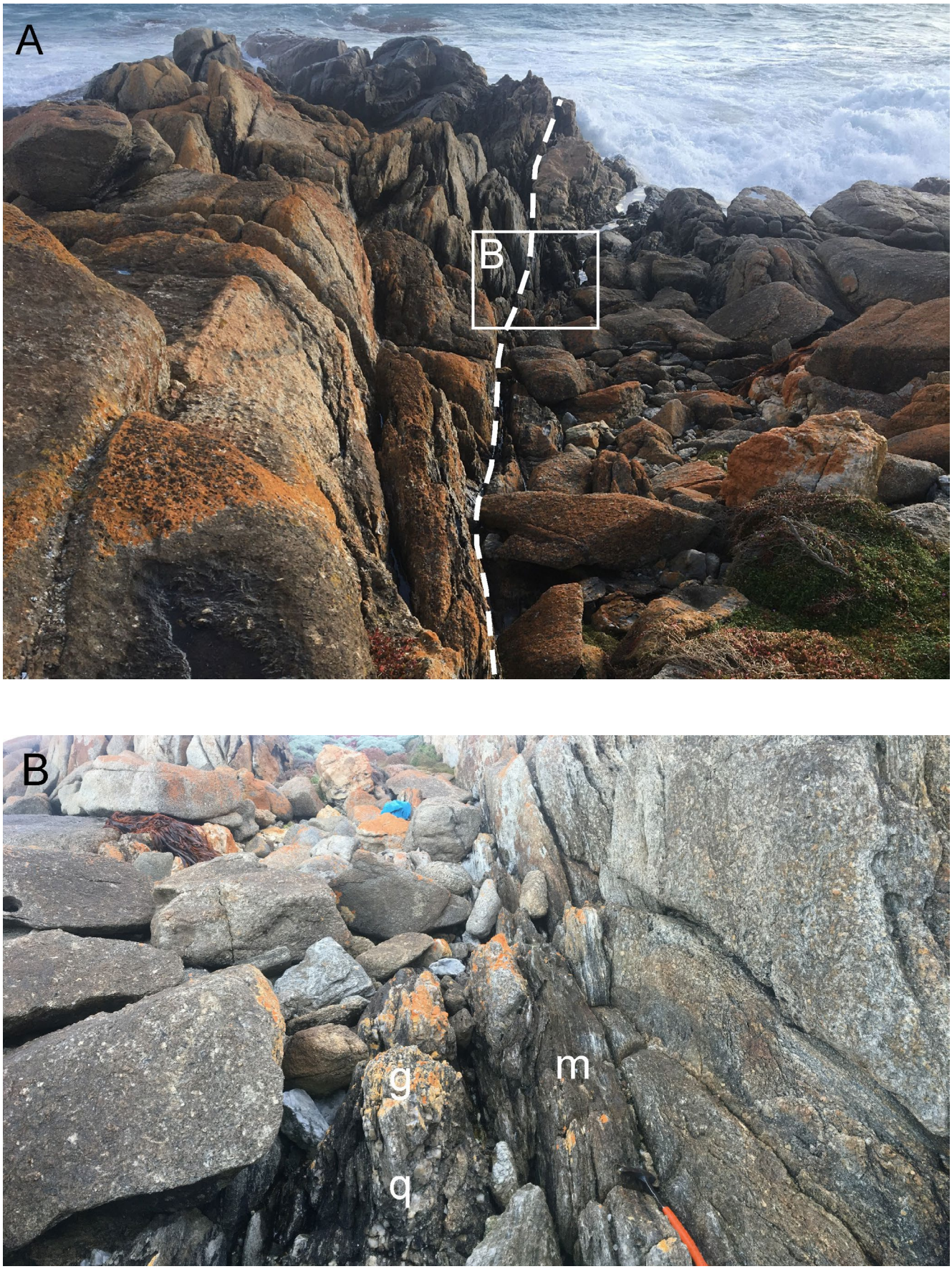

Figure 14. A. Rocky Point Shear Zone looking north with shear zone (dashed line) and location of image B. B. Looking south showing narrow mylonite zone (m) with highly foliated coarse-grained pegmatitic granite (g) and sigmoidal – fractured quartz veins (q) to the east of the high strain zone.

erately to steeply west (mylonitic fabric dipping ~75° to 270°). Streit (1994) reports a steeply south plunging mineral lineation with a west side up (reverse dextral) displacement. The eastern contact against porphyritic Cape Wickham Granite is sharp, and is followed to the east by 0.3 m of finely laminated mylonite, which passes further east into progressively less foliated but coarser grained pegmatitic granite. The easternmost extent of the shear zone is marked by discontinuous bands of milky-white lenticular to sigmoidal shaped and fractured quartz veins that are about 0.7 m thick.

5.3.1 Sample R030021 (mylonite)

Sample R030021 is a mylonite from the highest strain part of the Rocky Point Shear Zone. It contains 20% fractured and kinked feldspar (up to 1 mm) in a matrix dominated by recrystallised ribbon quartz (Figure 15). The matrix foliated, quartz dominated zone has bands with grains 100-200 µm wide and finer bands with quartz 10-20 µm in diameter that are rich in muscovite. K feldspar is partly replaced by muscovite. Khaki biotite is stable in the matrix. Undulose extinction and lobate boundaries are common in quartz. The Fe-Ti oxides have been replaced by epidote and titanite. Most of the plagioclase has been albitised.

There were 120 grains of REE phosphate detected up to 50 microns across. However, on closer inspection the monazite was highly altered and only a small part of these grains retained monazite compositions (Figure 16a). We obtained 8 valid analyses from these cores (Figure 5f) and they included 5 analyses with 1.3-2.2% Y that reflect the magmatic age of 766 ±40 Ma (MSWD=4.5). One valid analysis with low Y indicated resetting during an event at an age less than 630 Ma.

5.3.2 Sample R030022 (foliated granite)

Sample R030022 is a foliated granite sample from 2 m west of the shear zone. It shows very low strain features with K feldspar up to 1 cm, and a weak foliation. The original biotite is largely preserved. Fe-Ti oxide is converted to titanite and epidote, with extensive albitisation of plagioclase and moderate muscovite. The sample contains normal monazite content (1/3 of zircon content) with 76 grains detected up to 70 microns across.

Most of the analyses are from large grains with only minor evidence of fracture (e.g. Figure 16b). There were 7 spots slightly older than the magmatic (probably partially reset inherited grains) which provide an asymmetric shape to the age distribution (Figure 5g), and two spots that have been reset to lower ages, both on Grain 1 (Figure 16b). The twelve magmatic age spots are typical high-temperature monazite with up to 2 wt% Y and 2-6% Th. The weighted mean age for these spots is 758 ±15 Ma (MSWD=1.3).

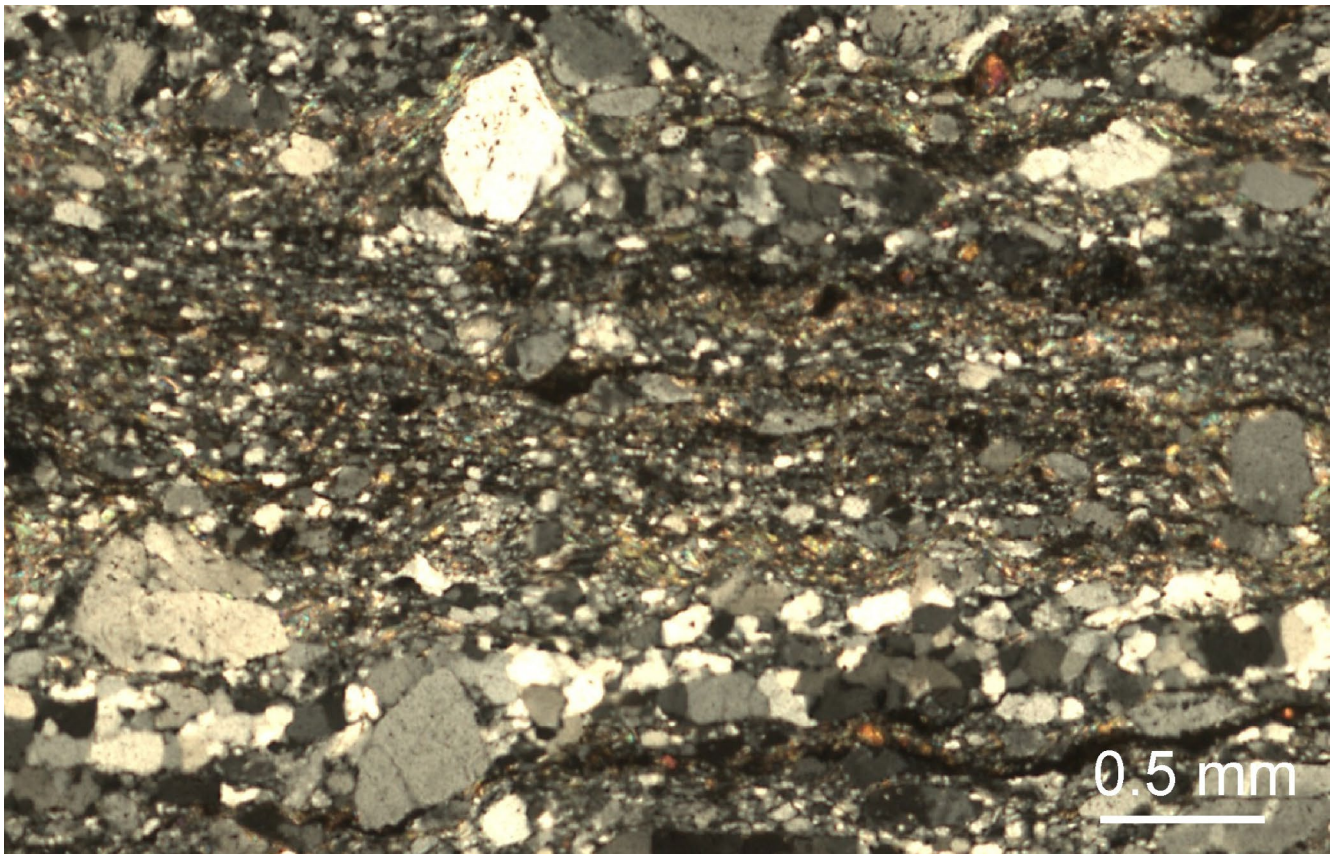

Figure 15. Texture of sample R030021 (cross polarised light), showing porphyroclasts of feldspar in very fine matrix of quartz and mica.

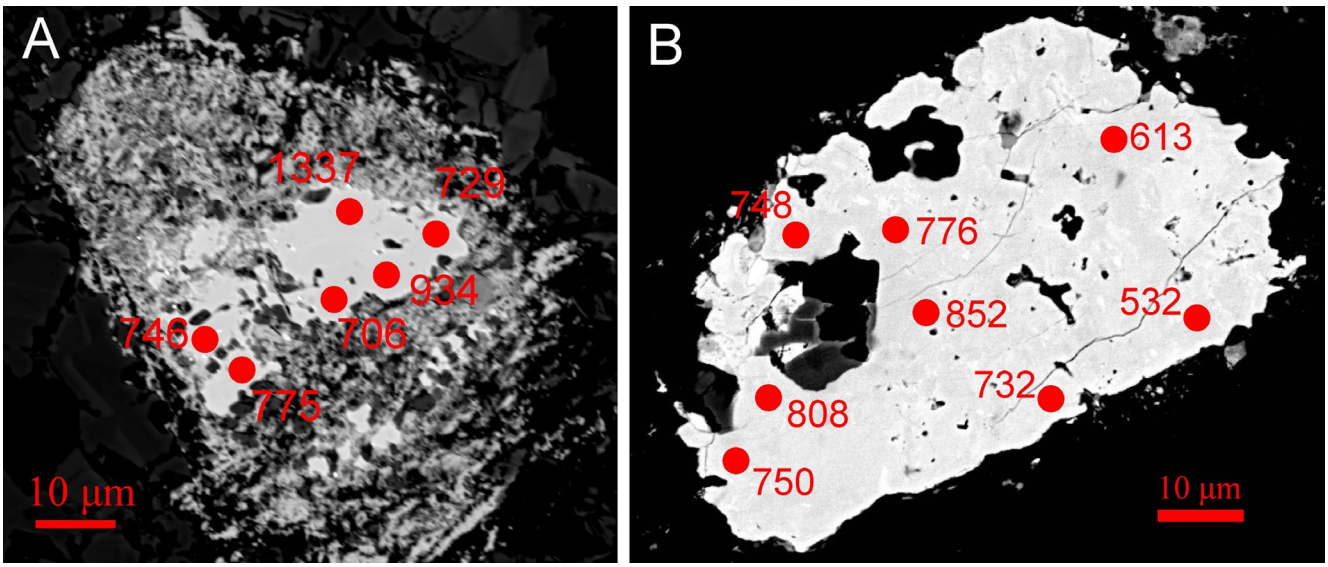

Figure 16. BSE image of A. grain 1 in sample R030021. Highly corroded monazite with fresh core retaining the magmatic age; B. largest grain in sample R030022 Ages shown in near analytical spots in red. Typical errors 20 Ma 1σ.

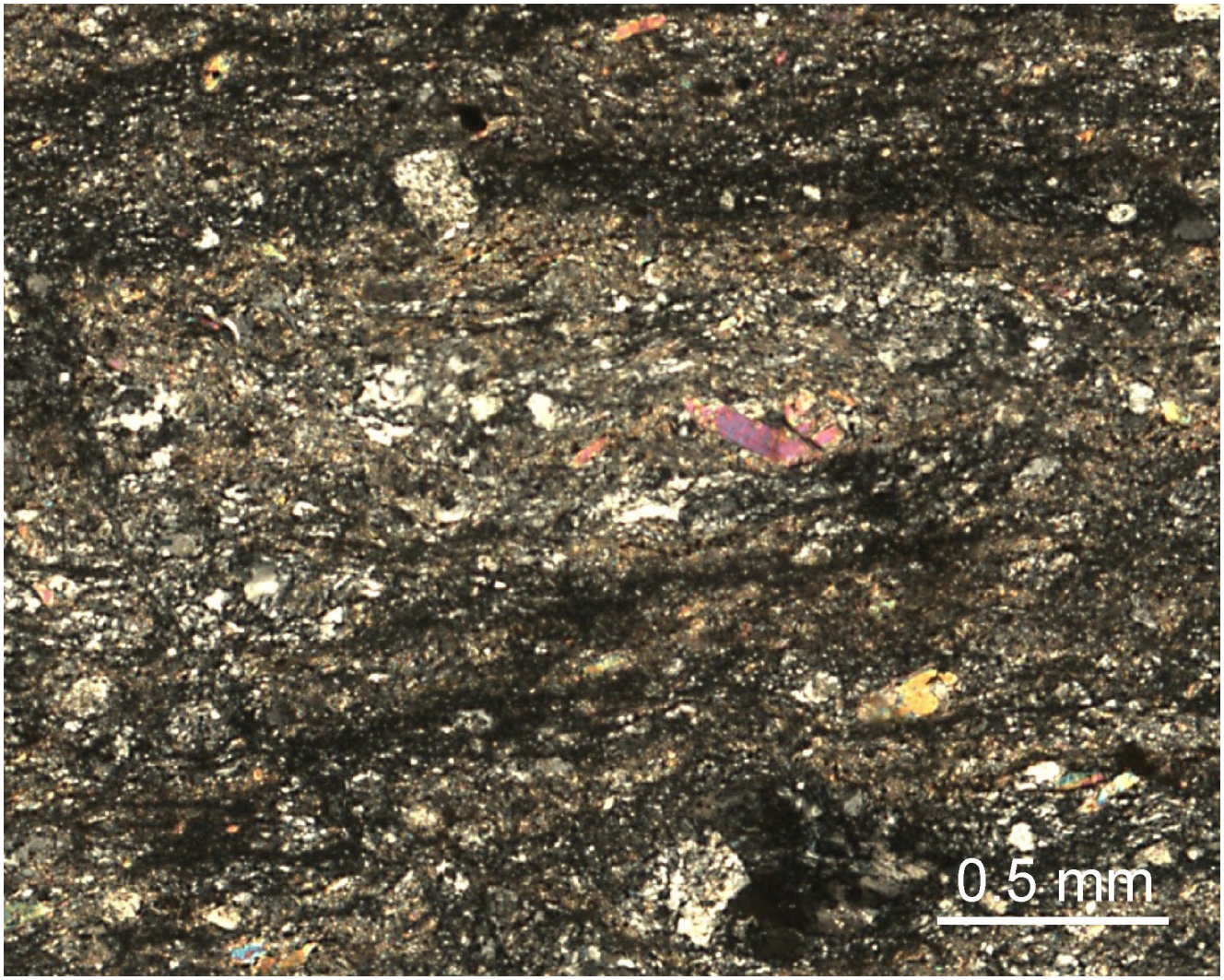

Figure 17. Texture of sample R014692 (cross polarised light), showing porphyroclasts of feldspar and porphyroblasts of muscovite overgrowing the foliation in very fine matrix of quartz and mica.

5.3.3 Summary

The Rocky Point Shear Zone strikes north and is subvertical with a steeply plunging lineation (Streit, 1994). There is evidence that final deformation was at lower temperature than the Cape Wickham Shear Zone, but otherwise they are very similar. Only three analyses were found to indicate deformation continued after 700 Ma. It is likely that the dominant mylonite formation event was close to the age of the granite, with minor reactivation after 550 Ma.

5.4 Currie Shear Zone

Currie Shear Zone outcrops discontinuously over 25 km along the west coast of King Island, from north of Currie to south of Cataraqui Point, with some segments offshore. Protoliths comprise the Surprise Bay Formation as well as the Loorana Granite. It is subvertical with evidence for multiple movement events including both dip slip and strike slip lineations at Currie, and oblique slip lineations at Cataraqui Point (Streit, 1994). The greater width and length of the Currie Shear Zone, compared to those in the north, suggest that this is a much larger fault than the shear zones on the north coast. Supporting this, it lies on the eastern flank of a much longer (>130 km) NNW-SSE-trending offshore magnetic anomaly which passes to within a few hundred metres of King Island at Surprise Point, where the zone of deformed rocks has its greatest width.

5.4.1 Sample R014692 (ultramylonite)

Sample R014692, from the northern side of a small gulch, 460 m north of Surprise Point, is a granite mylonite with a strong west-dipping penetrative foliation (57° to 269°). It is from a N-S-striking zone of intensely deformed Loorana Granite, at least 200 m wide. Sheared Surprise Bay Formation, with relict bedding, crops out about 100 m to the east (Figure 3f).

The sample is a white mica-rich ultramylonite (rare small porphyroclasts in a matrix that has domains of 20 µm and 10 µm grain size). The mineralogy is mainly quartz-albite-muscovite-chlorite. No biotite was seen. The bulk composition has lost Ca and some Na, with the main alteration being replacement of feldspar by muscovite. Muscovite is commonly boudinaged but other grains overgrow the foliation (Figure 17).

Eighty grains of REE phosphate were detected, with the largest four about 20 µm across. This was less than half of the abundance recognised in the previous samples. These grains have been deformed and show typical microboudinage features (Figure 18). All the grains are aligned in the foliation. They have a halo of low temperature minerals including rhabdophane, REE carbonates and rare xenotime reflecting reactions active during the deformation. While the grains have been deformed and fractured, the fractures have healed and the infill zones between grains are now monazite, indicating monazite was stable during the deformation. The new monazite is lower in Y than the original magmatic monazite.

Twenty-six successful analyses (Figure 5h) were carried out over five monazite grains. One analysis gave an age older than the granite age and is considered an inherited grain. The least deformed monazite has retained the magmatic age. In other areas the analyses show a mixed age reflecting partial resetting during recrystallisation below the closure temperature. The age spectra have a complex pattern with three nominal peaks including a magmatic age at 761 ±10 Ma (16 analyses MSWD=1.5). The second peak includes

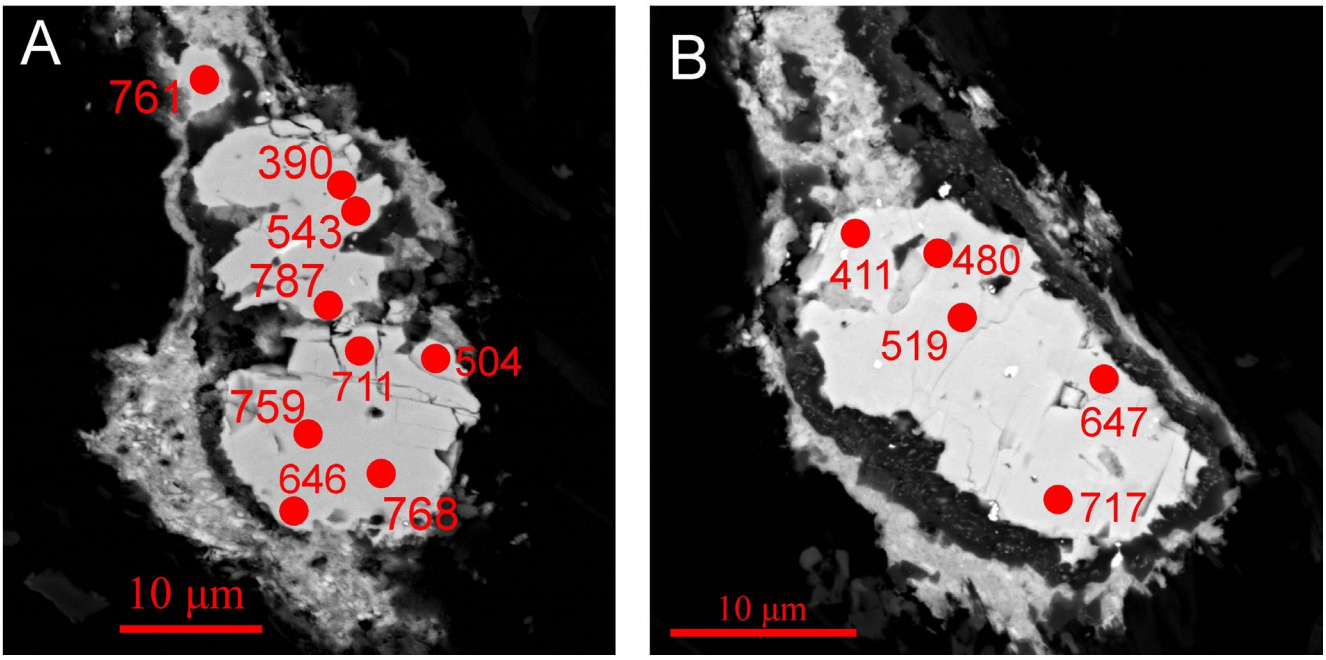

Figure 18. BSE images of monazite from sample R014692 (ultramylonite, Currie Shear Zone N of Surprise Point). A- grain 1, B- grain 3. Ages shown near analytical spots in red. Typical errors 20 Ma 1σ.

seven analyses with a nominal age of 533 ±43 Ma. The three youngest analyses indicate recrystallisation continued until at least 420 Ma. The parts of these grains that retain the "magmatic" age have a wide range of Y from 0.3 to 2.1 wt%. The areas of grains that have been reset to ages below 600 Ma are restricted to Y contents <0.8 wt%. The U in these grains is very low (<0.06%) unlike the Permian monazite in sample R029256. In comparison to metamorphic monazite, the "magmatic" age grains have Y contents typical of granites while the three lowest age grains all have compositions compatible with the white mica chlorite assemblage in this mylonitic sample. The analyses reflecting recrystallisation have higher LREE, lower HREE, and lower Th and U than the "magmatic" analyses.

The pattern of monazite ages is compatible with Palaeozoic reactivation of the Currie Shear Zone, probably during the Tyennan Orogeny (~500 Ma). The three analyses giving a younger age provide some evidence of further reactivation during the Devonian deformation.

5.5 Badger Box Creek Shear Zone

5.5.1 Sample R015724 (mylonite)

Strongly sheared grey-green granite crops out over an area of about 1.5 x 6 m at the head of a small gulch on the headland immediately south of the mouth of Badger Box Creek, ~ 5 km S of Currie (Figure 3d). The mylonitic fabric dips moderately east (~60° to 105°). Contacts here are obscured by sand, but ~30 m to the south, on the western side of the gulch, a continuation of the zone is ~1 – 2 m wide and is flanked by "normal" well-jointed, grey medium-grained, equigranular Loorana Granite. This small shear zone is subparallel to, but ~ 2-3 km east of, the much larger Currie Shear Zone, which here lies offshore.

Sample R015724 is texturally a mylonite (Figure 19) with 20% broken plagioclase crystals (0.5 mm) in a recrystallised quartz albite matrix (10-30 microns). The alteration is albitisation with Na enrichment and high epidote and chlorite. In bulk composition terms, the Ca, K and Rb are depleted and Na is enriched.

The rare phase search found one monazite grain which was too small to analyse. Nineteen very small xenotime (YPO_4) grains were detected approaching the minimum size limit for EPMA analysis. From these, the five largest grains were selected, and seven analyses were carried out using 1 µm beam size. The grains appear to be part of the equilibrium assemblage in this dark green foliated cataclasite. Two grains are interpreted as pressure shadows (Figure 20) suggesting the grains are syn-kinematic.

The xenotime grains vary compositionally with up to 2% Th and 0.2% U but only three analyses are above 1% Th. The textural evidence is that they crystallised at the same time, but the range in ages is larger than expected, giving a weighted average age of 430 ± 140 Ma (MSWD= 4). Of the grains with Th over 1%, one analysis gives an age of 531 ± 82 Ma consistent with a Cambrian deformation, and two analyses give an age of 366 ± 82 Ma consistent with Devonian deformation. The xenotime analyses indicate a late ductile movement on this shear zone but cannot distinguish whether it was at 500 Ma or 400 Ma. The variation in age results from individual spots is compatible with movement at both 500 Ma and 400 Ma.

6.0 Discussion

This study is largely about the age of shear zones cutting the Neoproterozoic granites of King Island. However, in seven samples an estimate of the granite age was also determined. These do not have the precision associated with the pre-existing zircon U-Pb results reported by Black et al. (2005) and Calver et al. (2013). They do confirm a consistent 760 Ma age for all samples that is within error of the previous U-Pb zircon results.

The Cape Wickham Shear Zone is a west dipping normal fault that Streit and Cox (1988) identified as a relatively high temperature shear zone. This is consistent with the samples reported here that are dominated by grain boundary migration textures. The movement vector on this shear zone was dip slip. The Rocky Point Shear Zone has a similar orientation with a steeply plunging lineation. A steeply plunging lineation was also found in the Currie Shear Zone, although there is much more evidence of reactivation in that example.

Streit and Cox (1998) concluded all the shear zones formed during a single main stage of mylonite formation based on the similarity of texture and mineralogy. The inferred deformation temperature of 400-500 °C indicates this event must be before 725 Ma (Figure 2). While the evidence for later reactivation is strong in the Currie and Disappointment Bay West shear zones, this textural argument also applies to them and the best explanation is that all these shear zones were formed while the temperature was above 400 °C. To search for evidence of this event we can look at the monazite analyses between 800 Ma and 700 Ma. There are 76 valid analyses in this range amongst all the samples. These must include all the magmatic compositions and those that formed during any mylonite event before 725 Ma. Magmatic grains usually have high Y content but monazite recrystallised below 500 °C is limited to Y less than 1% (Pyle et al., 2001). The calculated age from these analyses correlates with Y content (Figure 21). The twenty-five analyses with the highest Y (>1.86%) have a weighted average age of 759 ± 10 Ma (MSWD=2.5) while the 25 grains with the lowest Y (Y<1%) have a weighted average age of 740 ±9 Ma (MSWD=1.0). These two groups are different in age at the 95% confidence level based on a T test. The low

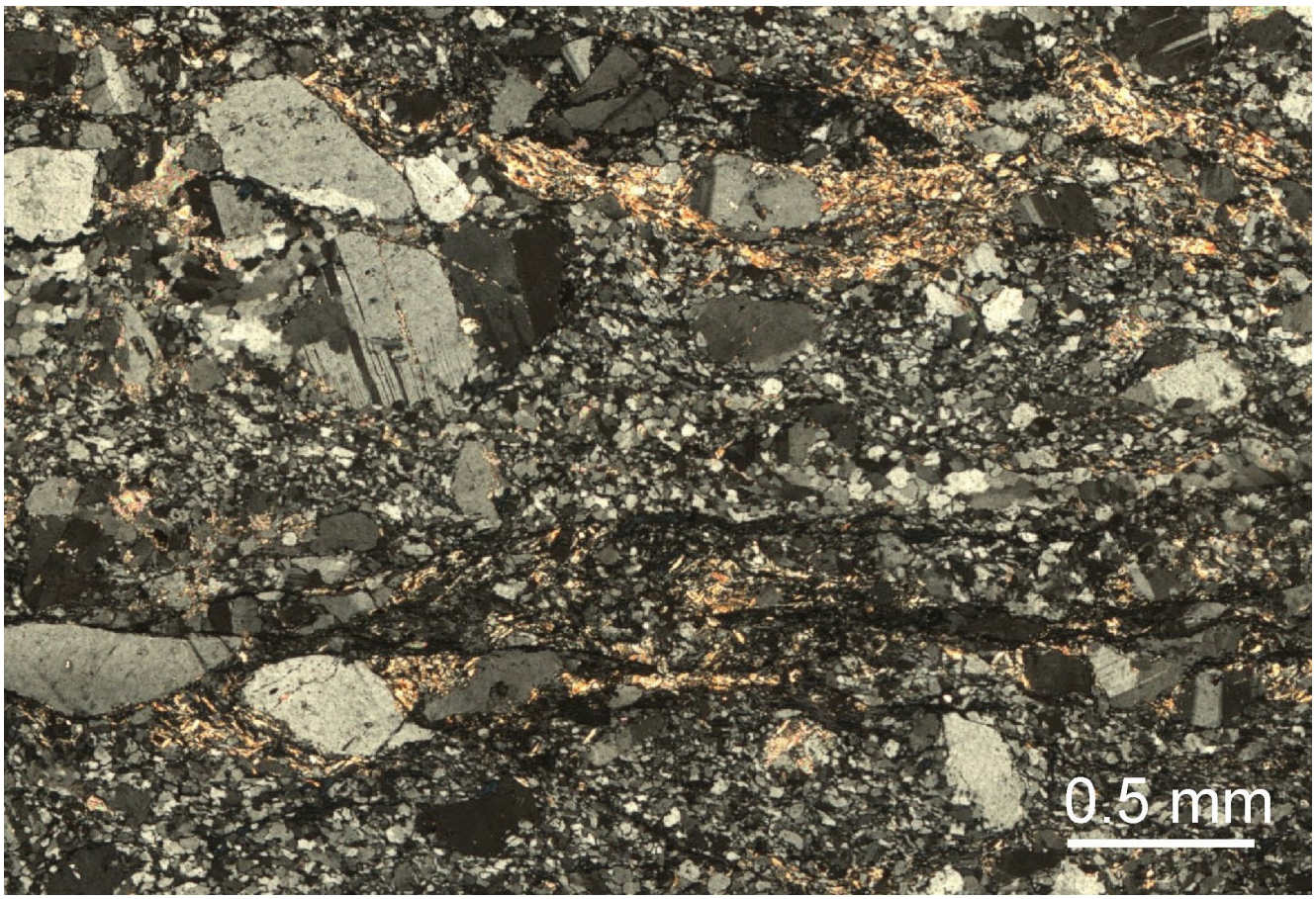

Figure 19. Texture of sample R015724 (cross polarised light), showing porphyroclasts of feldspar in a very fine matrix of quartz and mica.

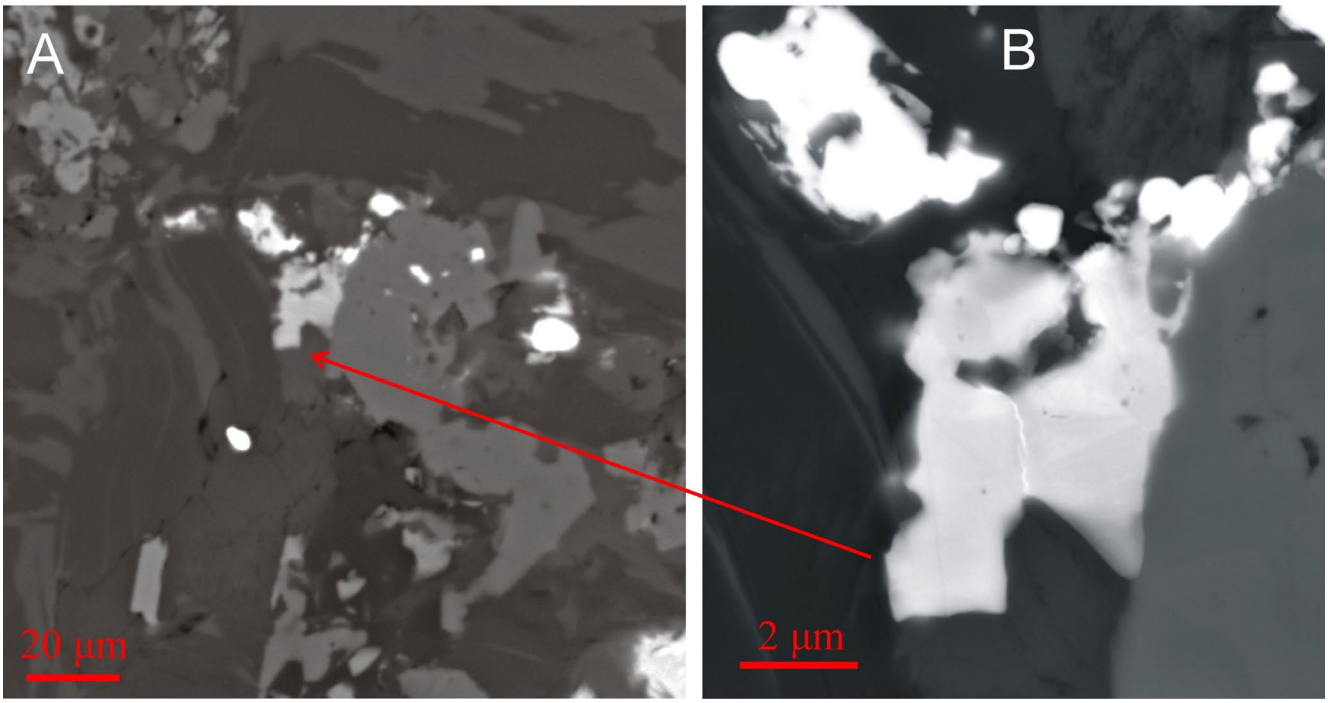

Figure 20. BSE image of xenotime grain 1 in sample R015724. A. larger area showing xenotime growing in the pressure shadow of titanite. B. detailed BSE image.

Y group has higher LREE's and a much smaller Eu anomaly (Eu/Eu*= 0.99) than the high Y group (Eu/Eu*= 0.67). The strong compositional shift is consistent with the interpretation that these analyses reflect recrystallised monazite compositions. The albitisation of plagioclase during mylonite formation releases extra Eu for inclusion in the monazite (cf. Didier et al., 2015). We conclude that the age of the major mylonite event is 740 ±9 Ma.

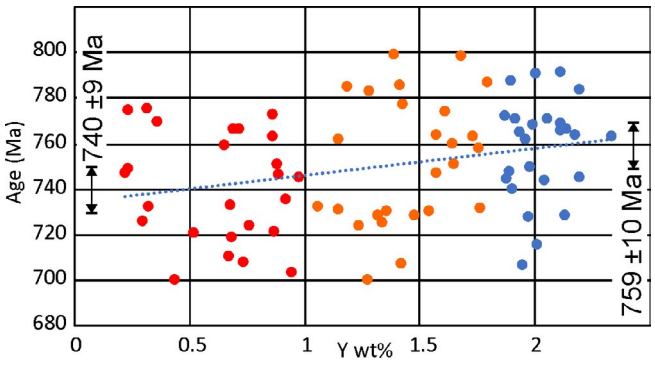

Figure 21. Age against monazite analyses in the range 800 to 700 Ma. Analyses less than 1% Y in red, and greater than 1.86% Y in blue.

The Disappointment Bay West Shear Zone is a moderately west dipping NNW striking mylonite zone with evidence of sinistral movement. Streit and Cox (1998) reported similar textures at Disappointment Bay to those of the Cape Wickham Shear Zone but noted more evidence of preserved subgrain structure and bulging grain boundaries which we interpret as evidence that the last significant ductile deformation was at lower temperature than the Cape Wickham Shear Zone. This is consistent with the lower temperature reported by Streit and Cox (1998) using the quartz K-feldspar $\delta^{18}O$ geothermometer (306 ±29 °C) for this shear zone. The monazite recrystallisation in the Disappointment Bay West Shear Zone indicated a preferred age for the reactivation of 500 Ma. Given this shear zone also has a different slip vector, we conclude that the Cambrian reactivation produced the sinistral strike slip movement on this fault.

The Currie Shear Zone also has sinistral strike slip movement indicators located near Currie (Streit, 1994). The sample from near Surprise Point shows evidence of low temperature reactivation and the recrystallised monazite suggests a 500 Ma age recrystallisation event. By analogy with the Disappointment Bay West Shear Zone, this is likely to be the time of the sinistral strike slip movement on this fault.

Sinistral movement of probable Cambrian age in a north striking, subvertical fault has not been reported before from King Island. Calver (2012) recognised a sub-vertical northeast striking cleavage in the Grassy Group along the east coast of King Island, which he concluded probably formed in the Cambrian. The implied NW-SE compression is consistent with the sinistral movement on the N-S striking faults studied in this project. The correlation of this cleavage with sinistral movement recorded on the Disappointment Bay West Shear Zone and the Currie Shear Zone provides further support for the conclusion that both events occurred in the Cambrian.

There is some evidence for later ductile reactivation in the Currie Shear Zone, which is likely to be Devonian since the rocks had cooled below 300 °C by 300 Ma (Figure 2). The extensive brittle reactivation (Streit, 1994) probably occurred after this Devonian event.

A later brittle movement on the Disappointment Bay West Shear Zone was associated with pyritic veins. The monazite that was recrystallised during this event gave an age of 293 ±15 Ma. Given the Grassy River Fault 50 km to the south (Figure 1) had a large sinistral offset after 350 Ma, we speculate these two events have the same age. Sinistral strike slip faults are a key feature of the New England Fold Belt and have typically been considered part of the Hunter Bowen Orogeny. However, Phillips et al. (2016) argued that the sinistral strike slip faulting occurred in the Early Permian (Asselian, 294-300 Ma) and before the Hunter Bowen Orogeny (265-230 Ma, Jessop et al., 2019). The Grassy River Fault and late brittle reactivation of the Disappointment Bay West Shear Zone may correlate with an early Permian sinistral transpression event along the eastern margin of Gondwana.

7.0 References

Berry R. F., Holm O. H. and Steele D. A. 2005. Chemical U–Th–Pb monazite dating and the Proterozoic history of King Island, southeast Australia. *Australian Journal of Earth Sciences,* 52, 461–471.

Black L. P., Seymour D.B., Corbett K.D., Cox S.E., Streit J.E., Bottrill R.S., Calver C.R., Everard J.L., Green G.R., McClenaghan M.P., Pemberton J., Taheri J. and Turner N.J. 1997. Dating Tasmania's oldest geological events. Australian Geological Survey Organisation Record 1997/15, 57pp.

Black L. P., Calver C. R., Seymour D. B. and Reed A. 2004. SHRIMP U-Pb detrital zircon ages from Proterozoic and Early Palaeozoic sandstones and their bearing on the early geological evolution of Tasmania. *Australian Journal of Earth Sciences,* 51, 885–900.

Black L. P., McClenaghan M. P., Korsch R. J., Everard J. L., and Foudoulis C. 2005. The significance of Devonian–Carboniferous igneous activity in Tasmania, as derived from U–Pb SHRIMP dating of zircon. *Australian Journal of Earth Sciences*, 52, 807–829.

Calver C. R. 2012. Explanatory report for the Grassy and Naracoopa geological map sheets. 1:25 000 Scale Digital *Geological Map Series — Explanatory Report,* 5, 69 pp.

Calver C.R. and Everard J.L. (compilers.) 2012. Digital Geological Atlas 1:25 000 Scale Series. *Sheet 2356 Pearshape*. Mineral Resources Tasmania.

Calver C. R., Meffre S. and Everard J. L. 2013. Felsic porphyry sills in Surprise Bay Formation near Currie, King Island, dated at ~775 Ma (LA-ICPMS, U-Pb on zircon). Tasmanian Geological Survey Record 2013/04, 10 pp.

Calver C. R. and Everard J. L. 2014. The Surprise Bay Formation (~1300 Ma) and related rocks of western King Island. Tasmanian Geological Survey Record 2014/01, 33 pp.

Carlson, R. W. 2011. *Absolute Age Determinations: Radiometric BT -Encyclopedia of Solid Earth Geophysics*, in Gupta, H.K. ed., Springer Netherlands, Dordrecht, p. 1–8.

Corbett K. D., Berry R. F., Everard J. L., Calver C. R., Crawford A. J., Vicary M. J., Bottrill R. S. and McNeill A. 2014. Cambrian Tasmania. In Corbett K. D., Quilty P. G. and Calver C. R. (eds). Geological Evolution of Tasmania. *Geological Society of Australia Special Publication,* 24, 95-240.

Cox S. F. 1973. *The structure and petrology of the Cape Wickham area, King Island*. BSc (Hons) thesis, University of Tasmania, Hobart (unpubl.).

Didier A., Bosse V., Bouloton J., Mostefaoui S., Viala M., Paquette J .L., Devidal J. L. and Duhamel R. 2015. NanoSIMS mapping and LA-ICP-MS chemical and U–Th–Pb data in monazite from a xenolith enclosed in andesite (Central Slovakia Volcanic Field). *Contributions to mineralogy and petrology,* 170: 45, 21 pp. DOI 10.1007/s00410-015-1200-1

Direen N. G., Jago, J. B. 2008. The Cottons Breccia (Ediacaran) and its tectonostratigraphic context within the Grassy Group, King Island, Australia: A rift-related gravity slump deposit. *Precambrian Research,* 165, 1–14.

Donovan, J. J., Snyder, D. A., and Rivers, M. A. 1993. An improved interference correction for trace element analysis. *Microbeam Analysis*, 2, 23–28.

Donovan, J. J., and Tingle, T. N. (1996). An improved mean atomic number background correction for quantitative microanalysis. *Journal of the Microscopy Society of America,* 2, 1–7.

Everard J. L. (compiler) 2011. Digital Geological Atlas 1:25 000 Scale Series. Sheet 2355 *Stokes*. Mineral Resources Tasmania.

Everard J. L. 2014. 3.7 Cryogenian (777-748 Ma) granitoids. In Corbett KD, Quilty PG and Calver CR (eds). Geological Evolution of Tasmania. *Geological Society of Australia Special Publication,* 24, 61-63.

Everard J. L. and Calver C. R. 2013a. Digital Geological Atlas 1:25 000 Scale Series. *Sheet 2357 Currie*. Mineral Resources Tasmania.

Everard J. L. and Calver C. R. (compilers.) 2013b. Digital Geological Atlas 1:25 000 Scale Series. *Sheet 2361 Wickham*. Mineral Resources Tasmania.

Gleadow A. J. W. and Lovering J. F. 1978a. Fission track geochronology of King Island, Bass Strait, Australia: Relationship to continental rifting. *Earth Planetary Science Letters*, 37, 429–437.

Gleadow A. J. W. and Lovering J. F. 1978b. Thermal history of granitic rocks from western Victoria: A fission-track dating study, *Journal of the Geological Society of Australia*, 25, 323-340.

Gresham J. J. 1972. The Regional Geology of King Island. Geopeko Ltd, King Island.

Grujic, D., Stipp M., and Wooden J. L. (2011), Thermometry of quartz mylonites: Importance of dynamic recrystallization on Ti-in-quartz reequilibration, *Geochemistry Geophysics Geosystems,* 12, Q06012, doi:10.1029/2010GC003368.

Holm O. H. 2002. Structural and metamorphic evolution of the Arthur Lineament, northwestern Tasmania, Australia. PhD thesis, University of Tasmania, Hobart (unpubl.).

Jercinovic, M. J., Williams, M. L., Allaz, J., and Donovan, J. J. (2012). Trace Analysis in EPMA. IOP Conference Series: *Materials Science and Engineering,* 32, 012012.

Jessop K., Daczko N. R. and Piazolo S. 2019. Tectonic cycles of the New England Orogen, eastern Australia: A Review, Australian Journal of Earth Sciences 66, 459-496, DOI: 10.1080/08120099.2018.1548378

Meffre, S., Direen, N. G., Crawford, A. J., Kamenetsky, V. 2004. Mafic volcanic rocks on King Island, Tasmania: Evidence for 579 Ma breakup in east Gondwana. Precambrian Research 135:177–191.

Montel J. M., Kato T., Enami M., Cocherie A., Finger F., Williams M., Jercinovic M. 2018. Electron-microprobe dating of monazite: The story. Chemical Geology, 484, 4-15. 10.1016/j.chemgeo.2017.11.001

Mulder, J. A., Everard, J. L., Cumming, G., Meffre, S., Bottrill, R. S., Merdith, A. S. and Cawood, P. A. (2020). Neoproterozoic opening of the Pacific Ocean recorded by multi-stage rifting in Tasmania, Australia. Earth-Science Reviews, 201, 103041. https://doi.org/10.1016/j.earscirev.2019.103041

Nagy G. and Draganits E., 1999. Occurrence and mineral-chemistry of monazite and rhabdophane in the Lower and ?Middle Austroalpine tectonic units of the southern Sopron Hills, (Austria). Mitt. Ges. Geol. Bergbaustud. Osterr. 42, 21–36.

Nagy G, Draganits E., Demeny A., Panto G. and Arkai P. 2002. Genesis and transformations of monazite, florencite and rhabdophane during medium grade metamorphism: examples from the Sopron Hills, Eastern Alps. Chemical Geology 191, 25– 46.

Oriolo S., Wemmer K., Oyhantcabal P., Fossen H., Schulz B. and Siegesmund S. 2018. Geochronology of shear zones – a review. Earth Science Reviews 185, 665-683.

Phillips, G., Robinson, J., Glen, R., and Roberts, J. (2016). Structural inversion of the Tamworth Belt: Insights into the development of orogenic curvature in the southern New England Orogen, Australia. Journal of Structural Geology 86, 224–240.

Pyle J. P., Spear F. S., Rudnick R. L., and McDonough W. F. (2001). Monazite xenotime garnet equilibrium in metapelites and a new monazite garnet thermometer. Journal of Petrology 42, 2083-2107.

Sack P. J., Berry R. F., Meffre S., Falloon T. J., Gemmell J. B. and Friedman R. M. 2011. In situ location and U-Pb dating of small zircon grains in igneous rocks using laser ablation–inductively coupled plasma–quadrupole mass spectrometry, Geochemistry Geophysics Geosystems 12, Q0AA14, doi:10.1029/2010GC003405.

Scott B. 1951: The petrology of the volcanic rocks of south east King Island, Tasmania. Papers and Proceedings of the Royal Society of Tasmania 1950, 113–136.

Snoke A. W., Tullis J. and Todd V. R. 1998. Fault related rocks, A photographic atlas. Princeton University Press, Princeton, 617 pp.

Streit J. E. 1994. Effects of fluid-rock interaction on shear zone evolution in Proterozoic granites on King Island, Tasmania. PhD thesis (unpubl.) ANU, Canberra, 255 pp.

Streit J. E. and Cox S. F. 1998. Fluid infiltration and volume change during mid-crustal mylonitization of Proterozoic granite, King Island, Tasmania. Journal of Metamorphic Geology 16, 197 – 212.

Turner N. J., Black L. P. and Kamperman M. 1998. Dating of Neoproterozoic and Cambrian orogenies in Tasmania. Australian Journal of Earth Sciences 45, 789–806.

Waldron H. M. and Brown A. V. 1993. Geological setting and petrochemistry of Eocambrian–Cambrian volcano-sedimentary rock sequences from southeast King Island, Tasmania. Record Tasmanian Geological Survey 1993/28.

APPENDICES

Located :
https://www.mrt.tas.gov.au/mrtdoc/dominfo/download/TR31/

Appendix 1 - Sample locations

-Download-

Appendix 2 - EPMA analyses of Monazite

-Download-

Appendix 3 - EPMA xenotime analyses

-Download-

Tasmanian
Government

Mineral Resources Tasmania
PO Box 56 Rosny Park
Tasmania Australia 7018
Ph: +61 3 6165 4800

info@mrt.tas.gov.au www.mrt.tas.gov.au